
THE COMPLEX INTERPLAY BETWEEN RISK TOLERANCE AND THE SPREAD OF INFECTIOUS DISEASES

Maximilian Nguyen
Lewis-Sigler Institute
Princeton University
Princeton, NJ 08544
mmnguyen@princeton.edu

Ari Freedman
Department of Ecology and Evolutionary Biology
Princeton University
Princeton, NJ, USA
arisf@princeton.edu

Matthew Cheung
Program in Applied and Computational Mathematics
Princeton University
Princeton, NJ, USA
matthew.cheung@princeton.edu

Chadi Saad-Roy
Miller Institute for Basic Research in Science
Department of Integrative Biology
University of California, Berkeley
Berkeley, CA, USA
csaadroy@berkeley.edu

Baltazar Espinoza
Biocomplexity Institute
University of Virginia
Charlottesville, VA, USA
baltazar.espinoza@virginia.edu

Bryan Grenfell
Department of Ecology and Evolutionary Biology
Princeton University
Princeton, NJ, USA
grenfell@princeton.edu

Simon Levin
Department of Ecology and Evolutionary Biology
Princeton University
Princeton, NJ, USA
slevin@princeton.edu

July 8, 2024

ABSTRACT

Risk-driven behavior provides a feedback mechanism through which individuals both shape and are collectively affected by an epidemic. We introduce a general and flexible compartmental model to study the effect of heterogeneity in the population with regards to risk tolerance. The interplay between behavior and epidemiology leads to a rich set of possible epidemic dynamics. Depending on the behavioral composition of the population, we find that increasing heterogeneity in risk tolerance can either increase or decrease the epidemic size. We find that multiple waves of infection can arise due to the interplay between transmission and behavior, even without the replenishment of susceptibles. We find that increasing protective mechanisms such as the effectiveness of interventions, the number of risk-averse people in the population, and the duration of intervention usage reduces the epidemic overshoot. When the protection is pushed past a critical threshold, the epidemic dynamics enter an underdamped regime where the epidemic size exactly equals the herd immunity threshold. Lastly, we can find regimes where epidemic size does not monotonically decrease with a population that becomes increasingly risk-averse.

Introduction

Recent outbreaks such as the COVID-19 pandemic, the 2014 Ebola outbreak, the 2009 influenza A (H1N1) pandemic, and the 2002 SARS epidemic brought to light many of the challenges of mounting an effective and unified epidemic response in a country as large and as diverse as the United States. Particularly during the COVID-19 pandemic, people were split in opinion on questions such as the origin of the virus [1], whether they would social distance or wear a mask [2–4], or whether the country should even have a pandemic response at all [5]. As time progressed, the situation became more dire and the death toll accumulated. People then had a new battery of questions to address, such as whether or not they would adhere to mandatory lock-downs [6–8] or whether they felt comfortable using the new mRNA vaccines [9, 10]. Compounding the issue were the multiple streams of information and potential misinformation spread through social media and other channels [11–14]. People’s stances on the questions and issues were diverse, arising from the milieu of differences in culture, geography, scientific education, sources of information, political leanings, and individual identity [15–17].

Taken altogether, these differences within the population reflect a spectrum of people’s risk tolerances to a circulating infectious disease. For any given intervention, such as social distancing, wearing a mask, or taking a vaccine, each person in the population falls somewhere on a spectrum of willingness to adopt the intervention. Given a threat level of an infectious disease in the population, some people will readily wear masks, whereas other people will refuse to.

In this study, we aim to analyze the impact of heterogeneity in risk tolerance and the resulting behavioral response on the dynamics of epidemics. We seek to add to a burgeoning literature on the impact of human behavior in epidemic response [18–31], which the recent pandemic highlighted as an area for further exploration in preparation for the next large scale global health crisis [32–34]. To study the impact of heterogeneity in risk tolerance on epidemic dynamics, we introduce a simple and flexible modeling framework based on ordinary differential equations that can be used for different interventions and an arbitrary partitioning of the population with regard to risk tolerance and behavioral responses. We will examine and discuss potential interesting outcomes that can arise from coupling individual-level preferences and population-level epidemiology.

Results

Model of Adaptive Intervention Usage under Heterogeneous Risk Tolerance

Here we assume people’s risk aversion manifests as the rate at which they adopt individual interventions in response to an infectious disease outbreak. The intuition underlying this paradigm is that more risk-averse individuals are more sensitive to becoming sick and thus will adopt interventions at a faster rate than more risk-tolerant people. We consider the following SPIR compartmental model of a population with n differing levels of risk tolerance (1-4). This model features four types of classes: unprotected susceptible (S), protected susceptible (P), infectious (I), and recovered with permanent immunity (R). Since there are n differing levels of risk tolerance, we subdivide the susceptible population into n discrete groups indexed by i , where $i \in \{1, 2, \dots, n\}$. Each tolerance level is characterized by an intervention adoption rate parameter (λ_i) and an intervention relaxation rate parameter (δ_i). Transitions of susceptibles between their unprotected class (S_i) and their corresponding protected class (P_i) are governed by the corresponding parameters of the same index (λ_i, δ_i). Overall, the system is governed by $3 + 2n$ parameters: a transmission rate parameter (β), a recovery rate parameter (γ), an intervention effectiveness parameter (ϵ), and an intervention adoption rate (λ_i) and intervention relaxation rate (δ_i) for each tolerance level.

$$\frac{dS_i}{dt} = -\beta S_i I - \lambda_i S_i I + \delta_i P_i \quad (1)$$

$$\frac{dP_i}{dt} = -(1 - \epsilon)\beta P_i I - \delta_i P_i + \lambda_i S_i I \quad (2)$$

$$\frac{dI}{dt} = -\gamma I + \sum_{i=1}^n (\beta S_i I + (1 - \epsilon)\beta P_i I) \quad (3)$$

$$\frac{dR}{dt} = \gamma I \quad (4)$$

The transition from the unprotected susceptible state to the protected susceptible state represents individuals implementing an intervention that confers them protection against disease transmission from an infected individual. The

rate at which intervention adoption occurs may be driven by individuals considering information such as the epidemic incidence rate (e.g. cases per day), the total number of infected individuals in the population (e.g. total number of active cases), and mortality rate (e.g. deaths per day) [22]. Here we assume that individuals have knowledge about the total number of infected individuals (I) and respond accordingly. Parameterizing each person's individual risk tolerance by λ_i , we assume each individual person adopts an intervention at a rate $\lambda_i I$. Then, if there are S_i number of people that behave exactly the same (i.e. have the same level of risk-aversion), then at the population scale there is a collective adoption rate of $\lambda_i S_i I$. The same reasoning holds for each of the n tolerance levels. We also consider a model where the adoption rate is driven by individuals reacting to the incidence rate (Supplemental Materials); while this produces a more complex mathematical model, the results are qualitatively similar.

The effectiveness of the intervention being used is captured by the parameter ϵ , which linearly scales down the transmission rate between infected and protected susceptibles. In the limit of $\epsilon = 1$, the intervention is perfectly effective and protected individuals cannot become infected. In the limit of $\epsilon = 0$ then the intervention is completely ineffective, which reduces the model to an SIR model without interventions. For simplicity, we assume each epidemic features only a single type of intervention (whether that be masking, social distancing, vaccines, etc.) and that the effectiveness of an intervention is identical across the population. In reality, multiple interventions may be available concurrently, which would drive additional variation in behavior due to differences in risk sensitivity across the population.

This model allows for protected individuals to relax their usage of interventions, becoming unprotected in the process. Here, individuals in the protected class can relax back to the unprotected class through two means, either through a rate that is dependent on the quantity of infections present or through a rate that is independent of the number of infections. The infection-dependent rate is implicitly captured through the λSI term, which can be thought of a net rate that can be further decomposed into adoption and relaxation rate terms (i.e. $\lambda SI = \lambda_{adoption} SI - \lambda_{relaxation} SI$). Here we have assumed the adoption term to always be greater than the relaxation term, otherwise individuals would never adopt an intervention. The infection-independent rate is governed by the intervention relaxation rate parameter (δ_i) for each tolerance level. In the limit of $\delta_i = 0$, an intervention is irreversible, which would represent an intervention such as vaccines with permanent immunity. When δ_i is non-zero, individuals are using interventions such as masking or social distancing. The infection-independent rate is motivated by factors such as psychological fatigue of social distancing [35, 36] and physical discomfort with wearing masks [37]. In general, we will consider the regime where the relaxation rate δ is of comparable scale or smaller than the transmission scale (i.e. $\delta \leq \beta$). This reflects intuition that people are likely to continue to protect themselves with interventions even beyond an initial outbreak [38].

For simplicity, we consider the model for the case when $n = 1$ and $n = 2$. A schematic for these two cases is shown in Figure 1. However, the framework is general and can be extended to any discrete number of groups.

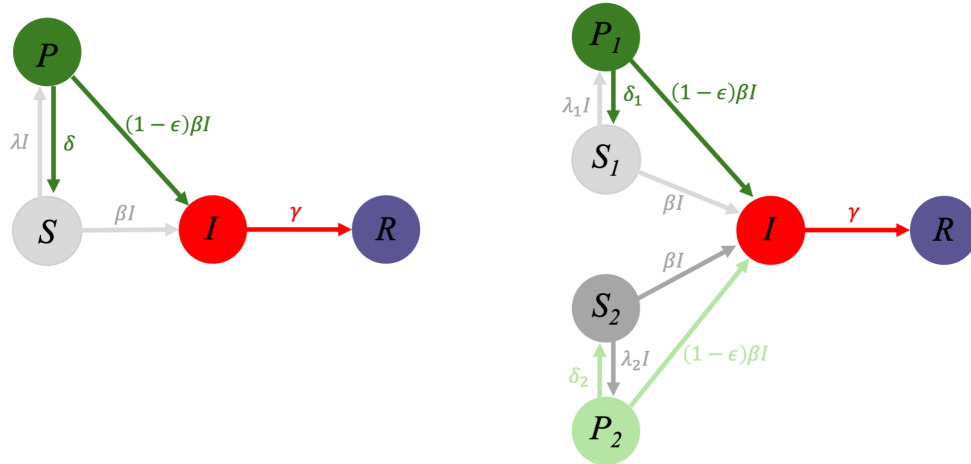


Figure 1: Flow diagram for an SIR model with adaptive interventions for either (a) a population with homogeneous risk tolerance or (b) a heterogeneous population with two different levels of risk tolerance. Susceptible individuals can access a more protected susceptible state through usage of interventions. The transition rate to the protected state depends on the incidence level. The protected state offers a $1 - \epsilon$ reduction in transmission rate over the normal susceptible state.

For convention, when there are two susceptible classes, we assume the first susceptible class (S_1) has a lower risk tolerance for becoming infected (i.e. more risk-averse). As a result, these individuals more readily adopt the intervention (i.e. $\lambda_1 > \lambda_2$), making individuals in this class transition more rapidly to the protected susceptible state

(P_1). The second susceptible class (S_2) is more risk tolerant (i.e. more risk-taking), and thus is less eager to use the intervention, making individuals in this class transition more slowly to their protected susceptible state (P_2).

Adaptive Adoption of Interventions Can Produce Damped Oscillations

The coupling of intervention usage to the incidence rate and the resulting adaptive changes enables the epidemic dynamics to display a much richer set of behavior over the simple SIR model. From Figure 2, we see this particular set of conditions can deterministically produce multiple waves of infection, even when vital dynamics (i.e. birth and death processes) are not considered.

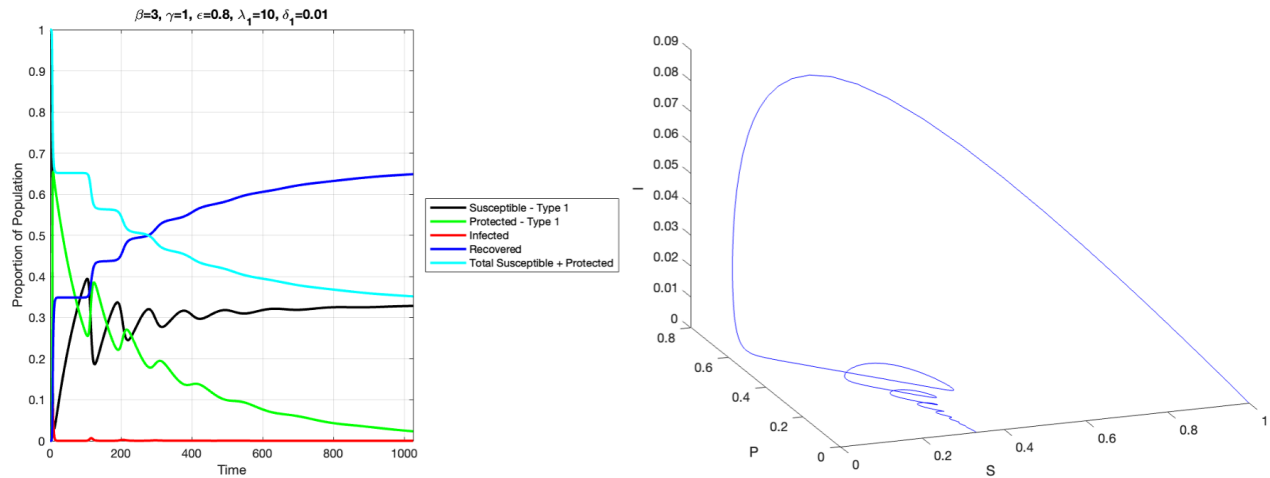


Figure 2: Time series for population with homogeneous risk tolerance and adaptive intervention usage and the corresponding phase space trajectory indicate the presence of damped oscillations.

Evidence for cycling of individuals between using interventions and not using interventions during the COVID pandemic can be seen in longitudinal usage [39–42] data. The possibility for these oscillations highlight the intimate connection between individual human behavior and intervention usage in shaping the dynamics of epidemics, while also be affected by the collective decision of everyone in the population. The coupling of behavior and epidemiology here provides a feedback mechanism where an increasing incidence rate prompts more individuals to adopt an intervention, which lowers the overall incidence rate; however, as the epidemic wanes and factors such as fatigue or discomfort set in, people begin dropping their usage of interventions, which may eventually lead to another wave of outbreaks if enough people become unprotected while infected individuals still remain, and then the cycle can be repeated.

Protective Mechanisms Saturate in Underdamped Regime that Eliminates Epidemic Overshoot

One might have the intuition that having more people that will more readily adopt an intervention (i.e. mask, social distance, or vaccinate) or increasing the effectiveness of the intervention in reducing transmission will further decrease the size of the epidemic. While we find this intuition to be mostly correct, we unexpectedly find that the protection conferred by either of these mechanisms can saturate once a critical parameter threshold has been passed.

In Figure 3, *left*, we see that increasing the effectiveness of the intervention or increasing the fraction of the population that are risk-averse monotonically decreases the epidemic size. However, in the dark blue region (which we will refer to as the underdamped regime) where both protection mechanisms are at their highest, we see no further reduction in the epidemic size. This regime corresponds to an epidemic where the epidemic size exactly equals the herd immunity threshold.

The orbits of the dynamics from different areas of this parameter space are shown in Figure 3, *right*. We see that even though the final epidemic size is the same throughout the underdamped region, the trajectories to reach the same final epidemic size can look qualitatively different.

Figures S4-S5 show a larger sampling of trajectories if one fixes either the fraction of the population with low risk tolerance or the intervention effectiveness respectively. It becomes clear that at the border of the underdamped region, we can see a clear change in the qualitative behavior of the trajectories as the threshold is crossed. Under some assumptions, one can prove that that the epidemic overshoot is eliminated in the underdamped regime (Supplemental Information).

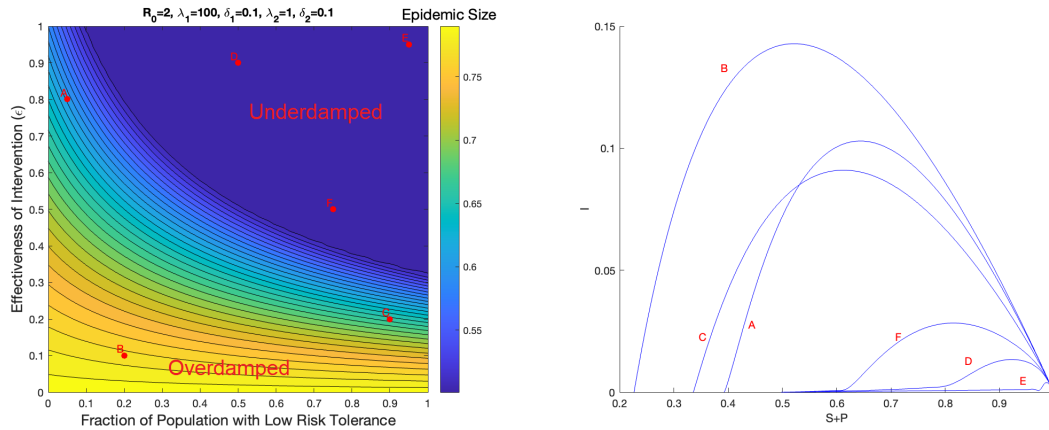


Figure 3: Left. Epidemic size as a function of varying the fraction of the population that are low-risk tolerance (i.e. those with higher λ). Right. Corresponding orbits in the I versus S+P plane for the sampled points in parameter space.

However, we should make the point that this is not evidence that highly effective interventions are a waste or that the overall population should tolerate risky behavior. As this is a model with a large parameter space, we cannot visualize all of it. If we could, we would find many parameter regimes where the protection mechanisms never reach a critical threshold, which implies the conventional intuition of increasing intervention effectiveness and having more risk-averse people always being beneficial applies.

The Threshold to the Underdamped Regime is Reduced when Intervention Usage is Prolonged

The transition to the underdamped regime is more easily accessed when the usage of interventions is prolonged (or equivalently when the rate at which protected individuals relax back into the regular susceptibility classes decreases). Consider the following scenario which is identical to the previous setup, except now the intervention reversion rate (δP_i) has been reduced by an order of magnitude (Figure 4). This corresponds to a scenario where people continue to use the intervention (i.e. such as wearing masks or social distancing) on a timescale significantly longer than the transmission timescale ($\delta \gg \beta$).

This suggests that increasing the timescale at which individuals continue to use interventions decreases the number of risk-averse individuals needed to achieve the same epidemic size. This is reflected in the horizontal shift of the transition region to the left when comparing figures in the left column and the right column (Figure 4).

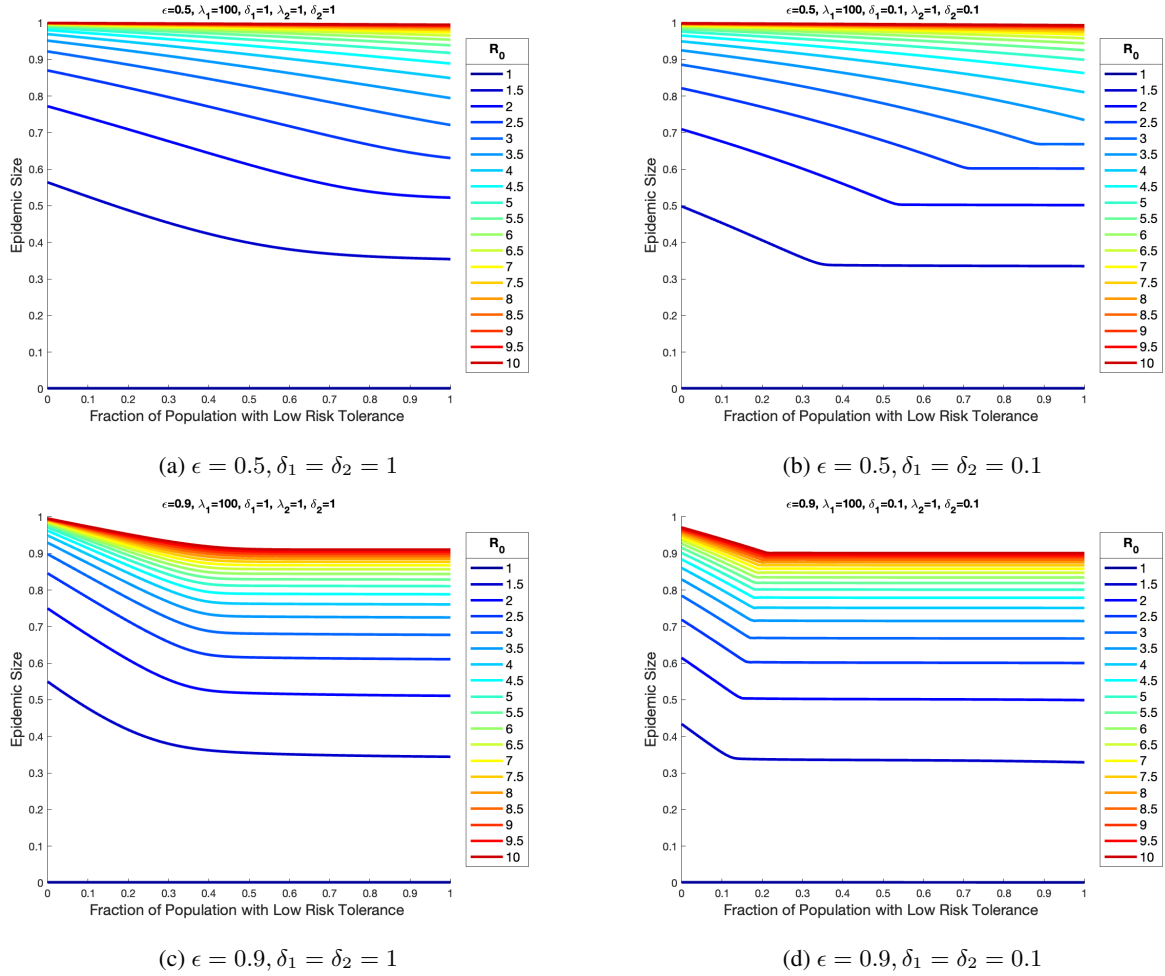


Figure 4: Final epidemic size versus fraction of population that are risk-averse (S_1). Simulations in the left column have a higher δ than simulations in the right column. The other simulation parameters and initial conditions are $\lambda_1 = 100, \lambda_2 = 1, I = 10^{-7}, P_1 = P_2 = 0, R = 0$.

Increasing Heterogeneity in Risk Tolerance can Either Increase or Decrease the Epidemic Size

The literature generally suggests that increasing heterogeneity in the population through increasing the variation in their contact patterns, age, etc. results in a reduction in the epidemic size [43–46].

We find in this model of heterogeneous behavior that it is possible to switch from a regime where increasing the heterogeneity in risk tolerance results in a decrease in epidemic size to a regime where increasing the heterogeneity in risk tolerance results in an increase in epidemic size. This result also does not have to necessarily be due to a dramatic shift in parameters. From Figure 5, we see this shift can arise from solely varying the fraction of the population with low risk tolerance by a small amount.

The intuition underlying this result is that when the average adoption rate ($\lambda_{average}$), which is expressed as a (geometric or arithmetic) weighted mean of the adoption rates of the two groups, is fixed at a constant level, then the epidemic size can be suppressed through either varying the fraction of the population in each group or through varying each group's adoption rate. When risk-averse people make up a smaller fraction of the population than risk-taking people, then it would be more beneficial in reducing epidemic size to have the adoption rates of the two groups be more similar (i.e. more homogeneous) as that would imply risk-taking people (which are then the majority of the population) would have a similar adoption rate to risk-averse people. As an increasingly larger fraction of the population is composed of risk-averse people, then it becomes increasingly beneficial in reducing epidemic size to have the adoption rates of the two groups be more different (i.e. more heterogeneous) as the deleterious effects of highly risk-taking people (which are then the minority of the population) can be mitigated by the large presence of risk-averse people.

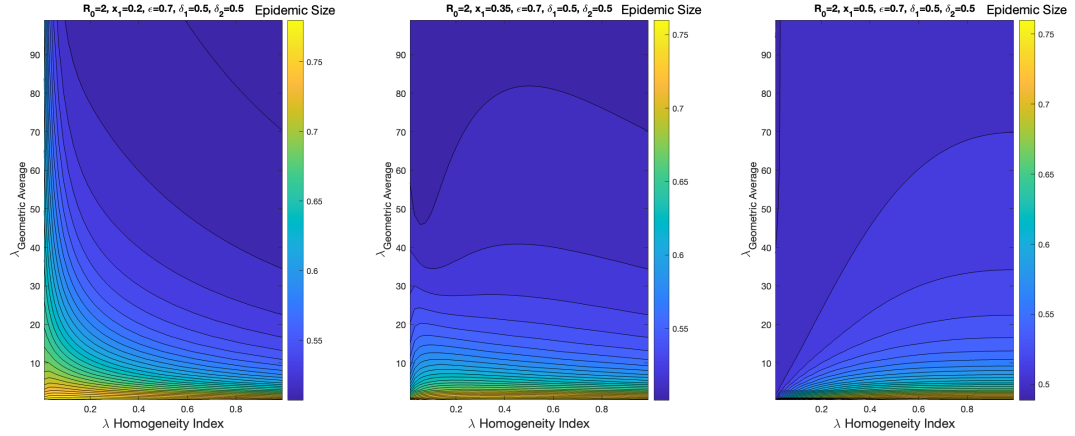


Figure 5: Epidemic size under differing levels of heterogeneity in the adoption rate for interventions. The mean adoption rate of the two groups (i.e. geometric average of λ_1, λ_2) is compared to the difference in the two adoption rates as parameterized by a homogeneity index (see Methods for definition). *Left* is when the fraction of the population with low risk tolerance (x_1) is 0.2, *center* is when $x_1 = 0.35$, *right* is when $x_1 = 0.5$.

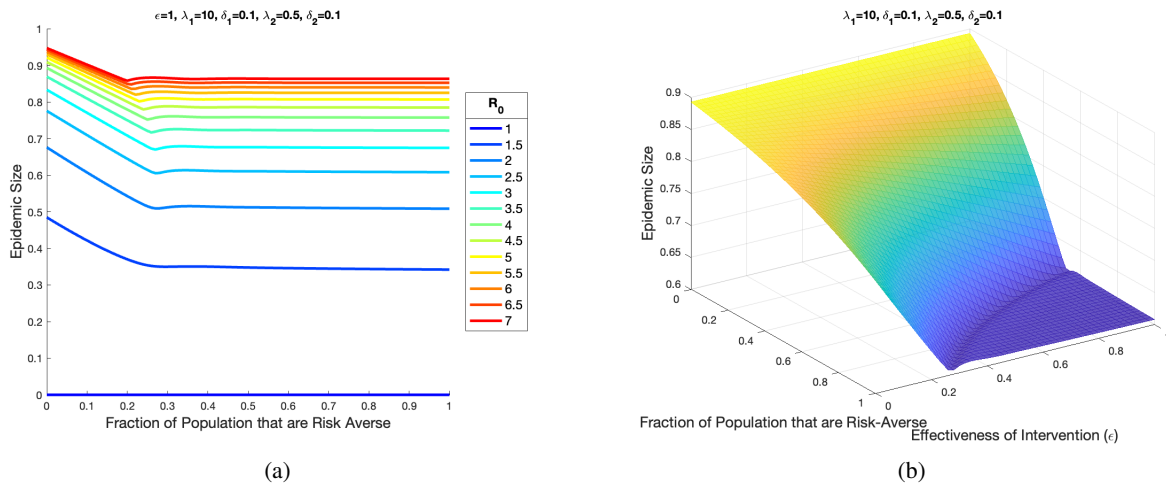


Figure 6: (a) Final epidemic size as a function of the proportion of the population that are risk averse (S_1). Model parameters and initial conditions for the simulation are $\epsilon = 1, \lambda_1 = 10, \lambda_2 = 0.5, \delta_1 = 0.1, \delta_2 = 0.1, I(0) = 10^{-7}, x_{S_2}(0) = 1 - x_{S_1} - I(0), P_1(0) = P_2(0) = 0, R(0) = 0$. (b) Same as in (a) except now the effectiveness of the intervention (ϵ) is allowed to vary.

Epidemic Size Does Not Necessarily Decrease with an Increasing Number of Risk-Averse People

General intuition would suggest that as one increases the number of risk-averse people in the population that the overall epidemic size would go down. However, the introduction of the adaptive behavior mechanism allows for regimes where this is no longer strictly the case. Thus, it is no longer a guarantee that decreasing the population's overall risk tolerance will always improve epidemic outcomes.

Consider Figure 6a, where we find a small region after the transition to the underdamped regime where there is an increase in the epidemic size when increasing the fraction of the population that are risk-averse.

If we also vary the effectiveness of the intervention as an additional axis (Figure 6b), we observe that there is a small trench in the threshold region surrounding the plateau area. This double descent suggests that the landscape can potentially be quite complicated when risk tolerance in the population is partitioned into even more groups.

Discussion and Conclusions

In this paper, we have proposed a simple model to model heterogeneity in risk tolerance levels in the population. We find that including a behavioral mechanism for adopting interventions that adapts with the level of infections greatly expands the variety in epidemic dynamics and outcomes that can occur.

The general picture from the findings suggest that epidemic dynamics under adaptive intervention adoption fall into either an underdamped regime or an overdamped regime. The underdamped regime has a special property in which the epidemic size equals the herd immunity threshold exactly, which means no epidemic overshoot occurs. The system can be driven into this regime when protection mechanisms (such as numbers of risk-averse people, intervention effectiveness, and duration of intervention usage) are increased to a sufficiently high level. This regime is also marked by damped oscillations in the phase space of infecteds and susceptibles. In direct contrast, the overdamped regime closely resembles the dynamics of a simple *SIR* model without behavior, in which there are no oscillations and a non-zero overshoot, which makes the epidemic size greater than the herd immunity threshold.

We have looked for some evidence in the historical data on outbreaks for these damped oscillations due to cycles in adoption and relaxation of interventions. While such data is in very limited supply, previous analysis suggested that relaxation of social distancing measures may have led to multiple waves of infection in the Spanish flu of the early 20th century [47, 48]. Dating back to the time of the bubonic plague, there is data from an outbreak in 1636 in the parish of St. Martin in the Fields, which showed how relaxation of quarantining and isolation measures lead to a smaller secondary wave of infections [49]. We also see some evidence from time-series data from early in the COVID pandemic on masking policy [40]. Taking mask policy as a proxy for the general level of mask usage [40], we can observe the policy level in the United States as it relates to the overall incidence in COVID infections during that same period [39], which we take as a rough proxy for the number of infected people. We see that a relaxation in the mask policy from its strictest level coincided with the rise of the Omicron variant soon afterward (Figure 7). While there are many confounding variables at play here including viral evolution that make it difficult to disentangle the contribution of individual factors, the timing suggests that behavior plays a key role in shaping the epidemic landscape as well.

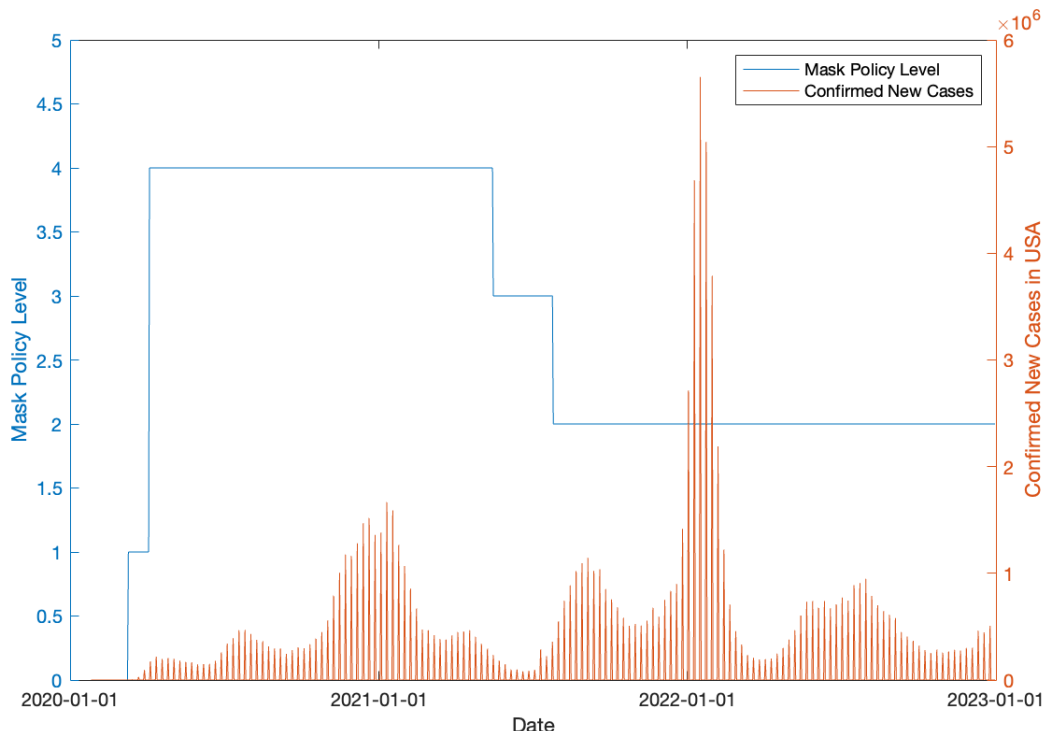


Figure 7: Time series data for masking policy and confirmed new cases in the USA for the first two years of the COVID pandemic. Data extracted from [39, 40].

The results here are reminiscent of feedback control systems commonly studied in control theory. Here the set point is the herd immunity threshold, which is determined by the basic reproduction number (R_0). The ability for the

population to reach this set point for epidemic size without additional overshoot depends on the effectiveness of the feedback mechanism from coupling intervention usage to the number of infected people. In the model presented, the adoption of interventions is a continuous process, in which the different groups are constantly reacting to the level of infections without requiring any notion of time or thresholds. In contrast, existing research on mitigation have considered more active control where activation and intervention timing play a key role [50–52]. Future work may explore how to synergistically utilize both active and continuous mechanisms for control.

The inclusion of heterogeneity in risk tolerance and adaptive adoption of interventions leads to several unexpected conclusions. We find that increasing heterogeneity in risk tolerance levels in the population can lead to either an increase or decrease in the epidemic size. The direction of the trend depends nonlinearly on the composition of the population in terms of the ratio of risk-averse to risk-taking individuals and their respective intervention adoption rates. This adds to a small literature that demonstrates how heterogeneity can actually lead to a larger epidemic [27, 53].

Interestingly, these results on heterogeneity also can be used to address the question of whether distributed or centralized control of mitigation results in a smaller outbreak. Control of factors such as mobility may be more practically achieved in a more centralized and unified fashion [54, 55], whereas a distributed approach may be more appropriate when considering factors such as speed and individual agency. In a centralized scenario, a single entity controls the dynamics. That situation has an exact correspondence to the homogeneous population considered here, where all individuals respond in unison. Distributed control allows for more localized control, such as individuals or small groups deciding if they want to mask or social distance. This corresponds to the heterogeneous scenarios considered here, where there are multiple groups each with differing risk tolerance level. The results suggest that in some scenarios a single, coordinated response would be better for mitigation, whereas in other parameter regimes, a more decentralized strategy would be more optimal.

We also find that increasing overall protection mechanisms does not always result in a monotonic decrease in epidemic size. In scenarios when the adoption rate begins to approach the transmission rate, near the critically damped boundary a nonmonotonicity can arise. This suggests that when intervention usage and effectiveness are tenuous, the dynamics become more complex and predicting what epidemic outcomes will result becomes significantly more difficult. Understanding how these nonlinear effects combine with other biological and behavioral heterogeneities will be important to explore in future work.

References

1. Maxmen, A. & Mallapaty, S. The COVID lab-leak hypothesis: what scientists do and don't know. *Nature* **594**, 313–315 (2021).
2. Betsch, C. *et al.* Social and behavioral consequences of mask policies during the COVID-19 pandemic. *Proceedings of the National Academy of Sciences* **117**, 21851–21853 (2020).
3. Fischer, C. B. *et al.* Mask adherence and rate of COVID-19 across the United States. *PLOS ONE* **16**, e0249891 (2021).
4. Yang, L. *et al.* Sociocultural determinants of global mask-wearing behavior. *Proceedings of the National Academy of Sciences* **119**, e2213525119 (2022).
5. Morens, D. M., Folkers, G. K. & Fauci, A. S. The Concept of Classical Herd Immunity May Not Apply to COVID-19. *The Journal of Infectious Diseases* **226**, 195–198 (2022).
6. Wong, C. M. L. & Jensen, O. The paradox of trust: perceived risk and public compliance during the COVID-19 pandemic in Singapore. *Journal of Risk Research* **23**, 1021–1030 (2020).
7. Brzezinski, A., Kecht, V., Van Dijke, D. & Wright, A. L. Science skepticism reduced compliance with COVID-19 shelter-in-place policies in the United States. *Nature Human Behaviour* **5**, 1519–1527 (2021).
8. Kleitman, S. *et al.* To comply or not comply? A latent profile analysis of behaviours and attitudes during the COVID-19 pandemic. *PLOS ONE* **16**, e0255268 (2021).
9. Machingaidze, S. & Wiysonge, C. S. Understanding COVID-19 vaccine hesitancy. *Nature Medicine* **27**, 1338–1339 (2021).
10. Fedele, F. *et al.* COVID-19 vaccine hesitancy: a survey in a population highly compliant to common vaccinations. *Human Vaccines & Immunotherapeutics* **17**, 3348–3354 (2021).
11. Gallotti, R., Valle, F., Castaldo, N., Sacco, P. & De Domenico, M. Assessing the risks of 'infodemics' in response to COVID-19 epidemics. *Nature Human Behaviour* **4**, 1285–1293 (2020).
12. Loomba, S., de Figueiredo, A., Piatek, S. J., de Graaf, K. & Larson, H. J. Measuring the impact of COVID-19 vaccine misinformation on vaccination intent in the UK and USA. *Nature Human Behaviour* **5**, 337–348 (2021).
13. Offer-Westort, M., Rosenzweig, L. R. & Athey, S. Battling the coronavirus 'infodemic' among social media users in Kenya and Nigeria. *Nature Human Behaviour*, 1–12 (2024).

14. Towers, S. *et al.* Mass Media and the Contagion of Fear: The Case of Ebola in America. *PLOS ONE* **10**, e0129179 (2015).
15. Murray, D. R. & Schaller, M. in *Advances in Experimental Social Psychology* (eds Olson, J. M. & Zanna, M. P.) 75–129 (Academic Press, 2016).
16. Kramer, P. & Bressan, P. Infection threat shapes our social instincts. *Behavioral Ecology and Sociobiology* **75**, 47 (2021).
17. Lu, J. G., Jin, P. & English, A. S. Collectivism predicts mask use during COVID-19. *Proceedings of the National Academy of Sciences* **118**, e2021793118 (2021).
18. Bansal, S., Grenfell, B. T. & Meyers, L. A. When individual behaviour matters: homogeneous and network models in epidemiology. *Journal of The Royal Society Interface* **4**, 879–891 (2007).
19. Funk, S., Salathé, M. & Jansen, V. A. A. Modelling the influence of human behaviour on the spread of infectious diseases: a review. *Journal of The Royal Society Interface* **7**, 1247–1256 (2010).
20. Fenichel, E. P. *et al.* Adaptive human behavior in epidemiological models. *Proceedings of the National Academy of Sciences* **108**, 6306–6311 (2011).
21. Edmunds, W. J., Medley, G. F. & Nokes, D. J. Evaluating the cost-effectiveness of vaccination programmes: a dynamic perspective. *Statistics in Medicine* **18**, 3263–3282 (1999).
22. Weitz, J. S., Park, S. W., Eksin, C. & Dushoff, J. Awareness-driven behavior changes can shift the shape of epidemics away from peaks and toward plateaus, shoulders, and oscillations. *Proceedings of the National Academy of Sciences* **117**, 32764–32771 (2020).
23. Wagner, C. E. *et al.* Economic and Behavioral Influencers of Vaccination and Antimicrobial Use. *Frontiers in Public Health* **8** (2020).
24. Tyson, R. C., Hamilton, S. D., Lo, A. S., Baumgaertner, B. O. & Krone, S. M. The Timing and Nature of Behavioural Responses Affect the Course of an Epidemic. *Bulletin of Mathematical Biology* **82**, 14 (2020).
25. Espinoza, B., Marathe, M., Swarup, S. & Thakur, M. Asymptomatic individuals can increase the final epidemic size under adaptive human behavior. *Scientific Reports* **11**, 19744 (2021).
26. Wagner, C. E., Saad-Roy, C. M. & Grenfell, B. T. Modelling vaccination strategies for COVID-19. *Nature Reviews Immunology* **22**, 139–141 (2022).
27. Espinoza, B., Swarup, S., Barrett, C. L. & Marathe, M. Heterogeneous adaptive behavioral responses may increase epidemic burden. *Scientific Reports* **12**, 11276 (2022).
28. Qiu, Z. *et al.* Understanding the coevolution of mask wearing and epidemics: A network perspective. *Proceedings of the National Academy of Sciences* **119**, e2123355119 (2022).
29. Traulsen, A., Levin, S. A. & Saad-Roy, C. M. Individual costs and societal benefits of interventions during the COVID-19 pandemic. *Proceedings of the National Academy of Sciences* **120**, e2303546120 (2023).
30. Saad-Roy, C. M. & Traulsen, A. Dynamics in a behavioral–epidemiological model for individual adherence to a nonpharmaceutical intervention. *Proceedings of the National Academy of Sciences* **120**, e2311584120 (2023).
31. Smith, R. A. *et al.* COVID-19 Mitigation Among College Students: Social Influences, Behavioral Spillover, and Antibody Results. *Health Communication* **38**, 2002–2011 (2023).
32. Morse, S. S. *et al.* Prediction and prevention of the next pandemic zoonosis. *The Lancet* **380**, 1956–1965 (2012).
33. Osterholm, M. T. in *The Covid-19 Reader* (Routledge, 2020).
34. Bergstrom, C. T. & Hanage, W. P. Human behavior and disease dynamics. *Proceedings of the National Academy of Sciences* **121**, e2317211120 (2024).
35. Franzen, A. & Wöhner, F. Fatigue during the COVID-19 pandemic: Evidence of social distancing adherence from a panel study of young adults in Switzerland. *PLOS ONE* **16**, e0261276 (2021).
36. Jørgensen, F., Bor, A., Rasmussen, M. S., Lindholt, M. F. & Petersen, M. B. Pandemic fatigue fueled political discontent during the COVID-19 pandemic. *Proceedings of the National Academy of Sciences* **119**, e2201266119 (2022).
37. Cheok, G. J. W. *et al.* Appropriate attitude promotes mask wearing in spite of a significant experience of varying discomfort. *Infection, Disease & Health* **26**, 145–151 (2021).
38. Barak, D., Gallo, E., Rong, K., Tang, K. & Du, W. Experience of the COVID-19 pandemic in Wuhan leads to a lasting increase in social distancing. *Scientific Reports* **12**, 18457 (2022).
39. Mathieu, E. *et al.* Coronavirus Pandemic (COVID-19). *Our World in Data* (2020).
40. Hale, T. *et al.* A global panel database of pandemic policies (Oxford COVID-19 Government Response Tracker). *Nature Human Behaviour* **5**, 529–538 (2021).
41. Rader, B. *et al.* Mask-wearing and control of SARS-CoV-2 transmission in the USA: a cross-sectional study. *The Lancet Digital Health* **3**, e148–e157 (2021).

42. Salomon, J. A. *et al.* The US COVID-19 Trends and Impact Survey: Continuous real-time measurement of COVID-19 symptoms, risks, protective behaviors, testing, and vaccination. *Proceedings of the National Academy of Sciences* **118**, e2111454118 (2021).
43. Miller, J. C. Epidemic size and probability in populations with heterogeneous infectivity and susceptibility. *Physical Review E* **76**, 010101 (2007).
44. Britton, T., Ball, F. & Trapman, P. A mathematical model reveals the influence of population heterogeneity on herd immunity to SARS-CoV-2. *Science* **369**, 846–849 (2020).
45. Gomes, M. G. M. *et al.* Individual variation in susceptibility or exposure to SARS-CoV-2 lowers the herd immunity threshold. *Journal of Theoretical Biology* **540**, 111063 (2022).
46. Allard, A., Moore, C., Scarpino, S. V., Althouse, B. M. & Hébert-Dufresne, L. The Role of Directionality, Heterogeneity, and Correlations in Epidemic Risk and Spread. *SIAM Review* **65**, 471–492 (2023).
47. Hatchett, R. J., Mecher, C. E. & Lipsitch, M. Public health interventions and epidemic intensity during the 1918 influenza pandemic. *Proceedings of the National Academy of Sciences* **104**, 7582–7587 (2007).
48. Caley, P., Philp, D. J. & McCracken, K. Quantifying social distancing arising from pandemic influenza. *Journal of The Royal Society Interface* **5**, 631–639 (2007).
49. Newman, K. L. S. Shut Up: Bubonic Plague and Quarantine in Early Modern England. *Journal of Social History* **45**, 809–834 (2012).
50. Bussell, E. H., Dangerfield, C. E., Gilligan, C. A. & Cunniffe, N. J. Applying optimal control theory to complex epidemiological models to inform real-world disease management. *Philosophical Transactions of the Royal Society B: Biological Sciences* **374**, 20180284 (2019).
51. Lauro, F. D., Kiss, I. Z. & Miller, J. C. Optimal timing of one-shot interventions for epidemic control. *PLOS Computational Biology* **17**, e1008763 (2021).
52. Morris, D. H., Rossine, F. W., Plotkin, J. B. & Levin, S. A. Optimal, near-optimal, and robust epidemic control. *Communications Physics* **4**, 1–8 (2021).
53. Volz, E. M., Miller, J. C., Galvani, A. & Meyers, L. A. Effects of Heterogeneous and Clustered Contact Patterns on Infectious Disease Dynamics. *PLOS Computational Biology* **7**, e1002042 (2011).
54. Bonaccorsi, G. *et al.* Economic and social consequences of human mobility restrictions under COVID-19. *Proceedings of the National Academy of Sciences* **117**, 15530–15535 (2020).
55. Espinoza, B., Castillo-Chavez, C. & Perrings, C. Mobility restrictions for the control of epidemics: When do they work? *PLOS ONE* **15**, e0235731 (2020).

Methods

Defining the λ Homogeneity Index

The λ homogeneity index is defined as follows. We will assume the initial condition that at the beginning of the dynamics, the total population is composed of the fraction of the population in the low risk tolerance group x_1 , the high risk tolerance group x_2 , or the infected class. We will assume the fraction of the population initially infected is sufficiently small so that size of the two susceptible compartments is given by x_1 and $1 - x_1$ respectively.

We can define the average adoption rate as being either a geometric or arithmetic mean of the two adoption rates. The choice one makes is arbitrary, so we present prescriptions for both routes. In both cases, we will map the level of homogeneity to the unit interval.

Geometric Average

Let the geometric average of the two adoption rates be given by $\lambda_{\text{Geometric Average}}$.

$$\lambda_{\text{Geometric Average}} = \lambda_1^{x_1} \lambda_2^{1-x_1} \quad (5)$$

Define λ_2 as a fraction between 0 and 1 of the average λ .

$$\lambda_2 = c \lambda_{\text{Geometric Average}}, c \in (0, 1] \quad (6)$$

These two equations combine to define λ_1 .

$$\lambda_1 = \frac{\lambda_{\text{Geometric Average}}}{c^{\frac{x_1}{1-x_1}}}, c \in (0, 1] \quad (7)$$

An index value of 1 indicates $\lambda_1 = \lambda_2$, while decreasing the index value towards 0 increases the difference between λ_1 and λ_2 .

Arithmetic Average

Let the arithmetic average of the two adoption rates be given by $\lambda_{\text{Arithmetic Average}}$.

$$\lambda_{\text{Arithmetic Average}} = x_1 \lambda_1 + (1 - x_1) \lambda_2 \quad (8)$$

Define λ_2 as a fraction between 0 and 1 of the average λ .

$$\lambda_2 = c \lambda_{\text{Arithmetic Average}}, c \in (0, 1] \quad (9)$$

These two equations combine to define λ_1 .

$$\lambda_1 = \frac{\lambda_{\text{Arithmetic Average}}(1 - x_1 c)}{1 - x_1}, c \in (0, 1] \quad (10)$$

Again, an index value of 1 indicates $\lambda_1 = \lambda_2$, while decreasing the index value towards 0 increases the difference between λ_1 and λ_2 .

Numerical Solutions and Code

Acknowledgements

M.M.N., A.S.F., M.A.C., and S.A.L. would like to acknowledge funding from NSF (CCF1917819, CNS-2041952, DMS-2327711), Army Research Office (W911NF-18-1-0325), and a gift from William H. Miller III. C.M.S.-R. acknowledges funding from the Miller Institute for Basic Research in Science of UC Berkeley via a Miller Research Fellowship. B.E.C. would like to acknowledge funding from NSF (IHBEM grant 2327710 and Expeditions NSF 1918656). B.T.G. would like to acknowledge the Princeton Catalysis Initiative and Princeton Precision Medicine.

Author Contributions

designed research, performed research, and wrote and reviewed the manuscript.

Additional information

Supplemental Material: The Complex Interplay Between Risk Tolerance and the Spread of Infectious Diseases

Analysis of the Model When Individuals Respond to the Incidence Rate

The rate at which intervention adoption occurs may be driven by individuals considering information such as the epidemic incidence rate (e.g. cases per day), the total number of infected individuals in the population (e.g. total number of active cases), and mortality rate (e.g. deaths per day) [22]. Here we will consider the first case, where individuals adopt interventions based on the incidence rate for infections. Recall that the incidence rate is given by $\sum_{i=1}^n (\beta S_i I + (1 - \epsilon)\beta P_i I)$. Parameterizing each person's individual risk tolerance by λ_i , let us assume each individual adopts an intervention at rate $\lambda_i \sum_{i=1}^n (\beta S_i I + (1 - \epsilon)\beta P_i I)$. Then, if there are S_i number of people that behave exactly the same (i.e. have the same level of risk-aversion), then at the population scale there is a collective adoption rate of $\lambda_i S_i \sum_{i=1}^n (\beta S_i I + (1 - \epsilon)\beta P_i I)$. The same reasoning holds for each of the n tolerance levels. The corresponding equations for this model are given by (11-14).

$$\frac{dS_i}{dt} = -\beta S_i I - \lambda_i S_i \sum_{i=1}^n (\beta S_i I + (1 - \epsilon)\beta P_i I) + \delta_i P_i \quad (11)$$

$$\frac{dP_i}{dt} = -(1 - \epsilon)\beta P_i I - \delta_i P_i + \lambda_i S_i \sum_{i=1}^n (\beta S_i I + (1 - \epsilon)\beta P_i I) \quad (12)$$

$$\frac{dI}{dt} = -\gamma I + \sum_{i=1}^n (\beta S_i I + (1 - \epsilon)\beta P_i I) \quad (13)$$

$$\frac{dR}{dt} = \gamma I \quad (14)$$

When comparing the final epidemic size and epidemic trajectories between this model and the model in the main text where individuals adopt interventions at a rate that is based on the total number of infected people (Figures S4-S5), the results are indistinguishable (Figures S1-S2).

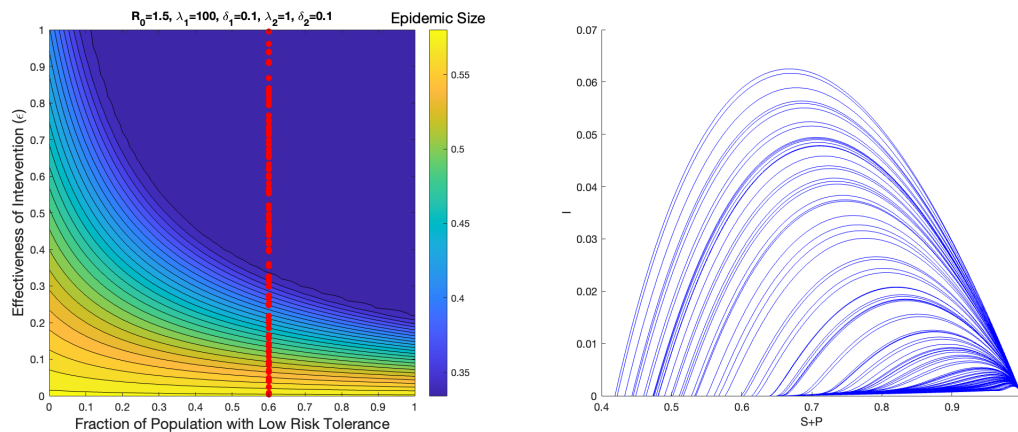


Figure S1: Left. Epidemic size as a function of varying the fraction of the population that are low-risk tolerance (i.e. those with higher λ) when individuals react to incidence rate. Right. Corresponding orbits in the I versus S+P plane for the sampled points in parameter space when the fraction of the population that are low-risk tolerance has been fixed.

Thus, given the equivalence in results, we have gone with the mathematically simpler and cleaner model based on total number of infected people in the main text.

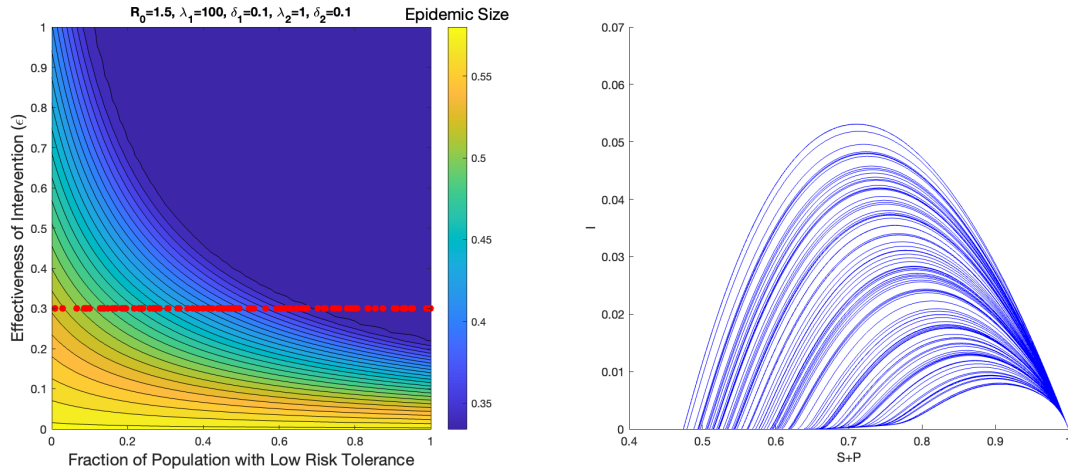


Figure S2: Left. Epidemic size as a function of varying the fraction of the population that are low-risk tolerance (i.e. those with higher λ) when individuals react to incidence rate. Right. Corresponding orbits in the I versus S+P plane for the sampled points in parameter space when the intervention effectiveness has been fixed.

The Herd Immunity Threshold is Set by a Complex Interplay Between Transmission (R_0), Behavior, and Intervention Effectiveness (ϵ).

While we could make some analytical calculations for the epidemic size in the homogeneous model, the heterogeneous two group case requires a numerical approach to find the plateau region. In general, it is set by a highly nonlinear interaction between the transmission (R_0), behavior as determined by the fraction of the population that are risk-averse and risk-taking, and the effectiveness of the intervention (ϵ).

Consider the following progression of figures (Figure S3), where in each subsequent figure, the effectiveness of the intervention in blocking transmission (ϵ) is increasing.

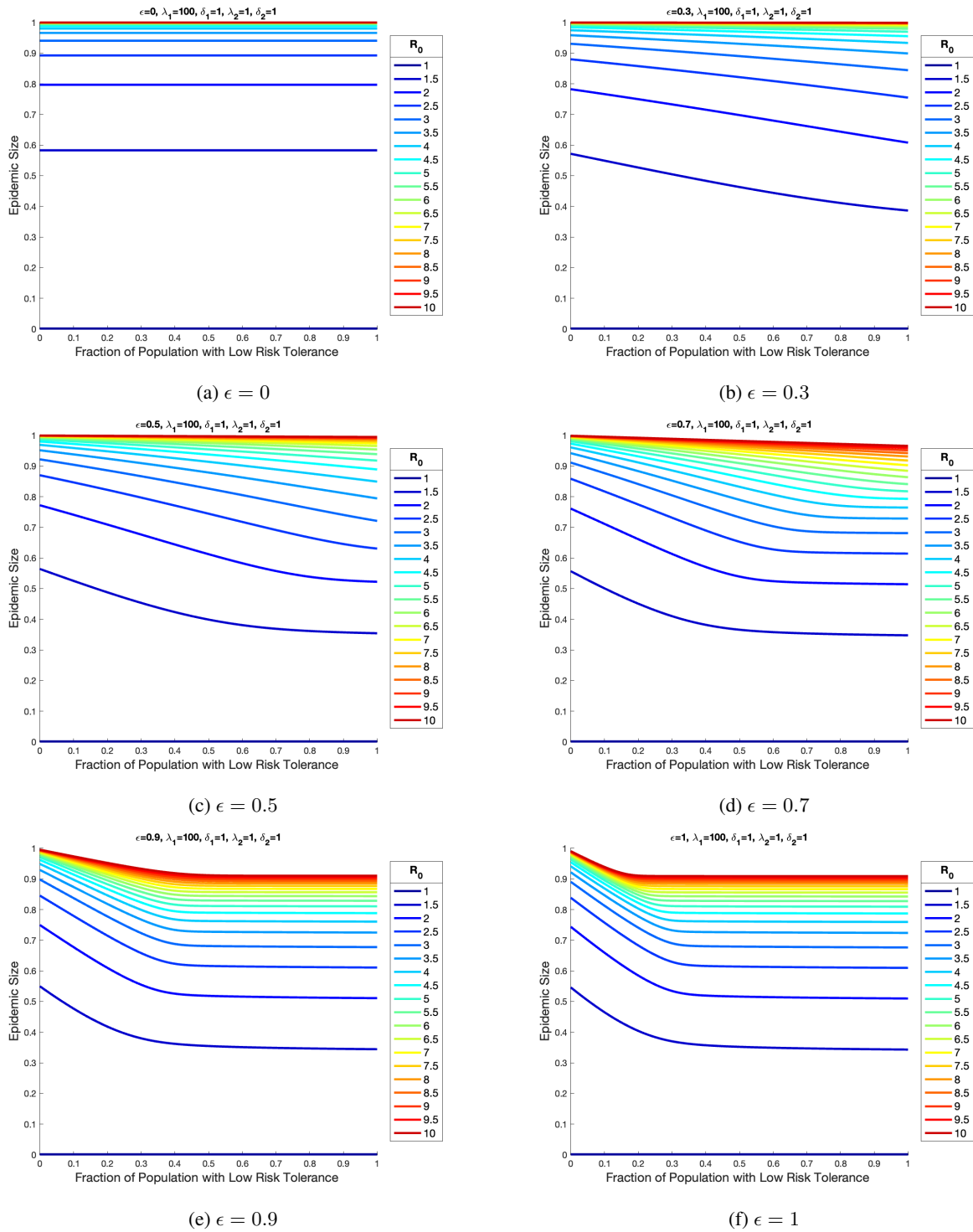


Figure S3: Final epidemic size versus fraction of population that are risk-averse (S_1) with a progressive increase in intervention effectiveness (ϵ). The other simulation parameters and initial conditions are $\lambda_1 = 100, \delta_1 = 1, \lambda_2 = 1, \delta_2 = 1, I(0) = 10^{-7}, P_1(0) = P_2(0) = 0, R(0) = 0$.

Comparing Orbits Inside and Outside of the Plateau Region of Herd Immunity

The following figures sample more orbits for the Figure considered in the main text.

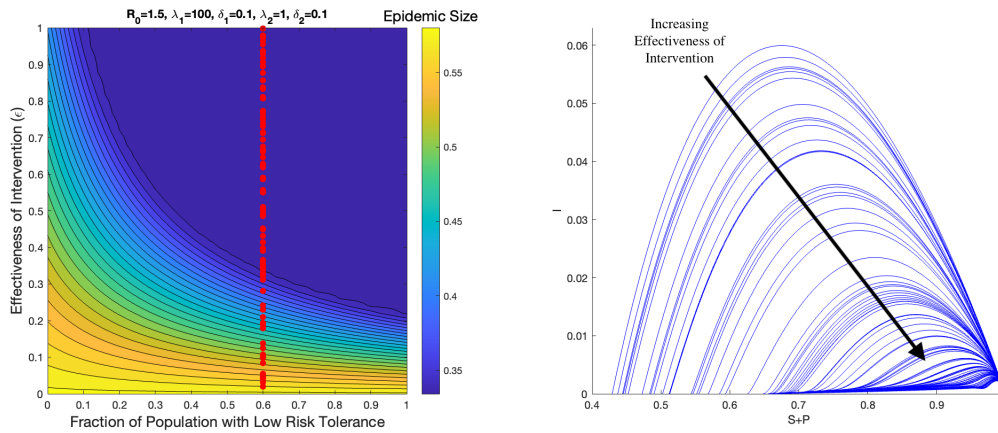


Figure S4: Left. Epidemic size as a function of varying the fraction of the population that are low-risk tolerance (i.e. those with higher λ). Right. Corresponding orbits in the I versus S+P plane for the sampled points in parameter space when the fraction of the population that are low-risk tolerance has been fixed.

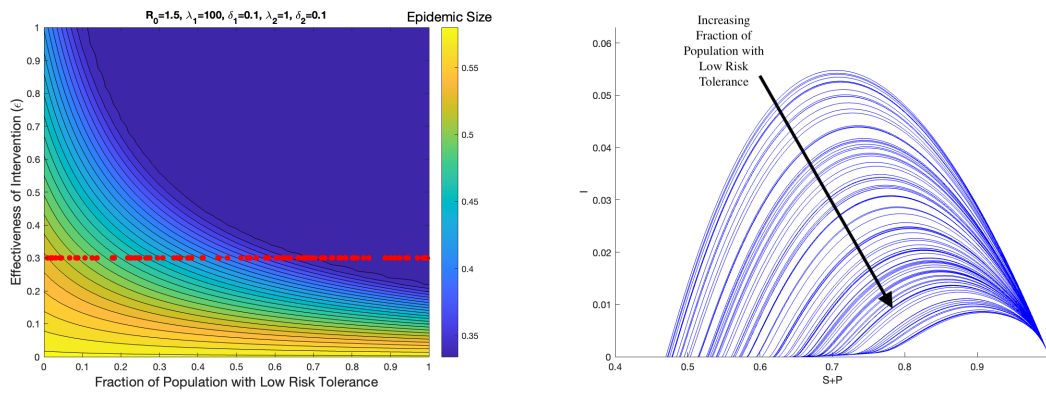


Figure S5: Left. Epidemic size as a function of varying the fraction of the population that are low-risk tolerance (i.e. those with higher λ). Right. Corresponding orbits in the I versus S+P plane for the sampled points in parameter space when the intervention effectiveness has been fixed.

Proving Underdamped Regime Eliminates Epidemic Overshoot

In general, the nonlinear feedback between the protected classes and infected individuals make it difficult to make analytical calculations in the full model. Under some simplifications however, we can make some progress. In this section, we derive the epidemic size at which the protection saturates in a restricted case of the homogeneous model ($n = 1$).

Let us consider the homogeneous model in the limit of an intervention with perfect effectiveness (i.e. $\epsilon = 1$). We will consider the case where the recovery rate from infection and relaxation rate for interventions are comparable (i.e. $\gamma = \delta$). Since the equation for recovered individuals can be ignored since the population is closed ($S + P + I + R = 1$), this reduces the dynamics to the following system:

$$\frac{dS}{dt} = -\beta SI - \lambda SI + \gamma P \quad (15)$$

$$\frac{dP}{dt} = \lambda SI - \gamma P \quad (16)$$

$$\frac{dI}{dt} = \beta SI - \gamma I \quad (17)$$

$$S(0) = f, P(0) = 0, I(0) = \alpha, R(0) = 1 - f - \alpha \quad (18)$$

The initial conditions sets the number of individuals initially susceptible to be f , the number of initially infected is assumed to be small $I(0) \ll 1$, and the remainder of the population is already immune to infection (i.e. recovered). To ensure that the epidemic initially grows in size, we assume that $S(0) > \frac{1}{R_0}$. This follows from comparing the incidence term (βSI) to the recovery term (γI) in 17.

To find the asymptotic behavior for S , we will attempt to eliminate P from (15). We start first by seeking an equation that relates the P and I compartments. Consider the following ansatz that considers the difference between the two compartments:

$$x = \frac{\beta}{\lambda} P - I \quad (19)$$

Differentiating this equation with respect to time and using (16)-(17) yields:

$$\frac{dx}{dt} = \gamma \left(I - \frac{\beta}{\lambda} P \right) \quad (20)$$

Using (19), this simplifies to $\frac{dx}{dt} = -\gamma x$, which has a critical point at $x = 0$. At $x = 0$, we obtain that $P = \frac{\lambda}{\beta} I$, indicating a regime where the behavior of P and I scale linearly with each other. Combining this with (15) yields:

$$\frac{dS}{dt} = \left(-(\beta + \lambda)S + \frac{\gamma\lambda}{\beta} \right) I \quad (21)$$

Now that we have an equation that is linear in I , we are in a good position to find a final size relationship for the number of susceptibles. To start we take the ratio of (17) and (21).

$$\frac{dI}{dS} = \frac{\beta SI - \gamma I}{\left(-(\beta + \lambda)S + \frac{\gamma\lambda}{\beta} \right) I} \quad (22)$$

Using the partial fractions $\frac{-\beta}{\beta + \lambda}$ and $\frac{\frac{\gamma\lambda}{\beta}}{\left((\beta + \lambda)S - \frac{\gamma\lambda}{\beta} \right)}$, we get upon indefinite integration of (22) that

$k = \frac{\beta}{\beta + \lambda} \left(\frac{\gamma}{\beta + \lambda} \ln \left((\beta + \lambda)S - \frac{\gamma\lambda}{\beta} \right) - S \right) - I$, where k is a constant that holds throughout the trajectory of the dynamics. Thus, considering the values of S and I at the beginning of the epidemic ($t = 0$) and the end of the epidemic ($t = \infty$) and using the conditions that $I(\infty) = 0$ and $I(0) \approx 0$ yields the following transcendental equation for the final epidemic size.

$$\frac{\beta}{\beta + \lambda} \left(\frac{\gamma}{\beta + \lambda} \ln \left((\beta + \lambda)S(0) - \frac{\gamma\lambda}{\beta} \right) - S(0) \right) = \frac{\beta}{\beta + \lambda} \left(\frac{\gamma}{\beta + \lambda} \ln \left((\beta + \lambda)S(\infty) - \frac{\gamma\lambda}{\beta} \right) - S(\infty) \right) \quad (23)$$

Since $S(0) > \frac{1}{R_0}$, then the argument of the logarithm on the left hand side must be positive, and subsequently the left hand side evaluates to a real number. Due to the equality, the right hand side must also evaluate to a real number,

implying the argument of the logarithm on the right hand side must also be positive. Positivity implies the following inequality for the lower bound for the final number of susceptibles:

$$S(\infty) > \frac{\gamma\lambda}{\beta(\beta + \lambda)} \quad (24)$$

An upper bound can be given by simply noting that in the long time limit, the recovery term (γI) must be at least as large as the incidence term ($\beta S(\infty)I$) in (17), otherwise the epidemic would still be growing. This implies $S(\infty) \leq \frac{1}{R_0}$.

To summarize, when the interventions are perfectly effective, the rate of relaxation from the protected class is equal to the rate of recovery from infection, and the number in the protected class scales linearly with the number of infected, then the final fraction of susceptibles is bounded as follows:

$$\frac{\lambda}{R_0(\beta + \lambda)} < S(\infty) \leq \frac{1}{R_0} \quad (25)$$

We see in the parameter limit of when the adoption rate of interventions is very fast compared to the transmission rate (i.e. $\lambda \gg \beta$), that the lower bound reduces to $\frac{1}{R_0}$. Since both bounds now coincide, then S_∞ must equal that value. Interestingly this corresponds to the herd immunity threshold of the standard SIR model. As the overshoot is the excess number of cases beyond the herd immunity threshold, we see that in this parameter limit there is no overshoot.

This analysis for the homogeneous case also carries over to the heterogeneous case for two groups when the adoption rate between the two groups is significantly different (i.e. $\lambda_1 \gg \lambda_2$). This results in a separation of time scales in which the faster adopters quickly transition to the protected state and can essentially be treated as immune over the course of the remaining epidemic over the slow adopters. This amounts to effectively reducing the dynamics to the homogeneous model considered here where f and $1 - f$ fractions of the population in the susceptible and recovered respectively correspond to the fraction of the population in the slow adopter (λ_2) and fast adopter groups (λ_1).

Heterogeneity in Risk Tolerance through Arithmetic Averaging

There are two ways for calculating the difference (heterogeneity) in adoption rates, either through geometric or arithmetic averaging. Both can be justified, and we presented the geometric formulation in the main text. We find that the arithmetic formulation gives qualitative similar results under a suitable parameter shift (Figure S6).

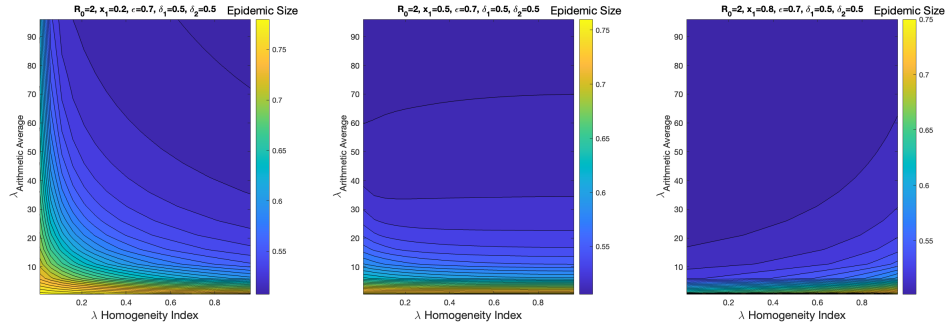


Figure S6: Epidemic size under differing levels of heterogeneity in the adoption rate for interventions. The mean adoption rate of the two groups (i.e. arithmetic average of λ_1, λ_2) is compared to the difference in the two adoption rates as parameterized by a homogeneity index (see Methods for definition). *Left* is when the fraction of the population with low risk tolerance (x_1) is 0.2, *center* is when $x_1 = 0.5$, *right* is when $x_1 = 0.8$.

Code to Generate Figures

Code executed in MATLAB R2023a.

```

1  %% %%%%%%%%%%%%%%%%%%%%%%%%%%%%%%%%%%%%%%%%%%%%%%%%%%%%%%%%%%%%%%%%%%%%%%%%%%% Functions
2  %% %%%%%%%%%%%%%%%%%%%%%%%%%%%%%%%%%%%%%%%%%%%%%%%%%%%%%%%%%%%%%%%%%%%%%%%%%%%
3  function totalRecovered = plotSIRDynamics(susceptibleFrac, R0,
4     transmissionReduction, PlotOption, gamma, lambda1, delta1, lambda2,
5     delta2, modelType)
6
7  % Initial conditions
8  initialInfected = 0.00000001;
9  initialSusceptible1 = susceptibleFrac;%(1-initialInfected)/2;
10 initialSusceptible2 = 1-initialInfected-initialSusceptible1;
11 initialMasked1 = 0;
12 initialMasked2 = 0;
13 initialRecovered = 0;
14
15 % Time vector
16 tspan = [0 10000];
17
18 % SIR ODE system
19
20 %% Reversible w/ total level response
21 sirODE_level = @(t, y) [
22     -beta*y(1)*y(5) - lambda1*y(1)*y(5) + delta1*y(2);
23     -beta*(1-transmissionReduction)*y(2)*y(5) - delta1*y(2) + lambda1*y(1)
24     *y(5);
25     -beta*y(3)*y(5) - lambda2*y(3)*y(5) + delta2*y(4);
26     -beta*(1-transmissionReduction)*y(4)*y(5) - delta2*y(4) + lambda2*y(3)
27     *y(5);
28     beta*(y(1)+y(3))*y(5) + beta*(1-transmissionReduction)*(y(2)+y(4))*y
29     (5) - gamma*y(5);

```

```

27     gamma * y(5)];
28
29 %% Reversible w/ incidence rate response
30
31 sirODE_incidence = @(t, y) [
32     -beta*y(1)*y(5) - lambda1*y(1)*(beta*(y(1)+y(3))*y(5) + beta*(1-
33     transmissionReduction)*(y(2)+y(4))*y(5)) + delta1*y(2);
34     -beta*(1-transmissionReduction)*y(2)*y(5) - delta1*y(2) + lambda1*y(1)
35     *(beta*(y(1)+y(3))*y(5) + beta*(1-transmissionReduction)*(y(2)+y(4)
36     )*y(5));
37     -beta*y(3)*y(5) - lambda2*y(3)*(beta*(y(1)+y(3))*y(5) + beta*(1-
38     transmissionReduction)*(y(2)+y(4))*y(5)) + delta2*y(4);
39     -beta*(1-transmissionReduction)*y(4)*y(5) - delta2*y(4) + lambda2*y(3)
40     *(beta*(y(1)+y(3))*y(5) + beta*(1-transmissionReduction)*(y(2)+y(4)
41     )*y(5));
42     beta*(y(1)+y(3))*y(5) + beta*(1-transmissionReduction)*(y(2)+y(4))*y
43     (5) - gamma*y(5);
44     gamma * y(5)];
45
46 % Solve ODE
47 if modelType == 1
48     [t, y] = ode89(sirODE_level, tspan, [initialSusceptible1;
49     initialMasked1; initialSusceptible2; initialMasked2;
50     initialInfected; initialRecovered]);
51 else
52     [t, y] = ode89(sirODE_incidence, tspan, [initialSusceptible1;
53     initialMasked1; initialSusceptible2; initialMasked2;
54     initialInfected; initialRecovered]);
55 end
56
57 if PlotOption == 1
58     % Plot results
59     figure;
60     plot(t, y(:, 1), 'k-', 'LineWidth', 2, 'DisplayName', 'Susceptible -
61     Type 1');
62     hold on;
63     plot(t, y(:, 3), 'b-', 'LineWidth', 2, 'DisplayName', 'Susceptible -
64     Type 2');
65     plot(t, y(:, 2), 'g-', 'LineWidth', 2, 'DisplayName', 'Protected -
66     Type 1');
67     plot(t, y(:, 4), 'm-', 'LineWidth', 2, 'DisplayName', 'Protected -
68     Type 2');
69     plot(t, y(:, 5), 'r-', 'LineWidth', 2, 'DisplayName', 'Infected');
70     plot(t, y(:, 6), 'b-', 'LineWidth', 2, 'DisplayName', 'Recovered');
71     plot(t, y(:, 1)+y(:, 2)+y(:, 3)+y(:, 4), 'k.', 'LineWidth', 2, '
72     DisplayName', 'Total Susceptible + Protected');
73     xlabel('Time');
74     ylabel('Proportion of Population');
75
76     ylim([0 1])
77     title(['\beta=', num2str(beta), ', \gamma=', num2str(gamma), ', \epsilon='
78     , num2str(transmissionReduction), ', \lambda_1=', num2str(lambda1), '
79     , \delta_1=', num2str(delta1), ', \lambda_2=', num2str(lambda2), ', \
80     delta_2=', num2str(delta2), ', x_{S_1}=', num2str(susceptibleFrac)]);
81     legend('Location', 'eastoutside');
82     grid on;
83     hold off;
84
85 end

```

```

67
68 if PlotOption == 2
69     hold on
70     plot(y(:, 1)+y(:,2)+y(:, 3)+y(:,4), y(:,5), 'b-')
71     xlabel('S+P')
72     ylabel('I')
73     ylim([0 .15])
74 end
75
76 totalRecovered = y(end,6);
77 end
78
79 %% %%%%%%%%%%%%%%%%%%%%%%%%%%%%%%%%%%%%%%%%%%%%%%%%%%%%%%%%%%%%%%%%%%%%%%%%%%%%%%% Script
80 %% %%%%%%%%%%%%%%%%%%%%%%%%%%%%%%%%%%%%%%%%%%%%%%%%%%%%%%%%%%%%%%%%%%%%%%%%%%%%%%%
81 %%%%%%%%%%%%%%%%%%%%%%%%%%%%%%%%%%%%%%%%%%%%%%%%%%%%%%%%%%%%%%%%%%%%%%%%%%%%%%% Figure 2 %%%%%%%%%%%%%%%%%%%%%%%%%%%%%%%%%%%%%%%%%%%%%%%%%%%%%%%%%%%%%%%%%%%%%%%%%%%%%%%
82
83 %%%% SIR model parameters
84 R0 = 3; % Basic reproduction number
85 gamma = 1; % Recovery rate
86 beta = R0*gamma; % Transmission rate of unmasked susceptibles
87 transmissionReduction = 0.8; % Effectiveness of intervention (\epsilon)
88 lambda1 = 10; % Rate parameter for unprotected susceptibles to adopt
      intervention
89 delta1 = .01; % Rate parameter for protected individuals to remove
      intervention (mask)
90
91 PlotOption = 1; % Plotting parameter. If 1, then plot graph, otherwise
      none.
92
93 % Initial conditions
94 initialInfected = 0.000001; % Seed fraction of population that are
      initially infected
95 initialSusceptible1 = 1-initialInfected;
96 initialMasked1 = 0;
97 initialRecovered = 0;
98
99 % Time vector
100 tspan = [0 1500];
101
102 % SIR ODE system
103 %% Reversible w/ total level response
104 sirODE_level = @(t, y) [
105     -beta*y(1)*y(3) - lambda1*y(1)*y(3) + delta1*y(2);
106     -beta*(1-transmissionReduction)*y(2)*y(3) - delta1*y(2) + lambda1*y(1)
      *y(3);
107     beta*y(1)*y(3) + beta*(1-transmissionReduction)*y(2)*y(3) - gamma*y(3)
      ;
108     gamma * y(3)];
109
110 % Solve ODE
111 [t, y] = ode89(sirODE_level, tspan, [initialSusceptible1; initialMasked1;
      initialInfected; initialRecovered]);
112
113 if PlotOption == 1
114     % Plot results
115     figure;
116     plot(t, y(:, 1), 'k-', 'LineWidth', 2, 'DisplayName', 'Susceptible -
      Type 1');

```

```

117     hold on;
118     plot(t, y(:, 2), 'g-', 'LineWidth', 2, 'DisplayName', 'Protected -
      Type 1');
119     plot(t, y(:, 3), 'r-', 'LineWidth', 2, 'DisplayName', 'Infected');
120     plot(t, y(:, 4), 'b-', 'LineWidth', 2, 'DisplayName', 'Recovered');
121     plot(t, y(:, 1)+y(:, 2), 'c-', 'LineWidth', 2, 'DisplayName', 'Total
      Susceptible + Protected');
122     xlabel('Time');
123     ylabel('Proportion of Population');
124     ylim([0 1])
125     title(['\beta=', num2str(beta), ', \gamma=', num2str(gamma), ', \epsilon='
      , num2str(transmissionReduction), ', \lambda_1=', num2str(lambda1), ',
      \delta_1=', num2str(delta1)]);
126     legend('Location', 'eastoutside');
127     grid on;
128     hold off;
129     %
130     %     saveas(gcf, ['NPImodel_', 'beta', num2str(beta), '_gamma', num2str(gamma)
      , '_epsilon', num2str(transmissionReduction), '_lambda1-', num2str(lambda1)
      ], '_delta1-', num2str(delta1), '.png'])
131
132     figure
133     hold on
134     plot3(y(:, 1), y(:, 2), y(:, 3), 'b-')
135     xlabel('S')
136     ylabel('P')
137     zlabel('I')
138 end
139
140 totalRecovered = y(end, 4);
141
142
143 %%%%%%%%%%%%%%%%%%%%%%%%%%%%%%%%%%%%%%%%%%%%%%%%%%%%%%%%%%%%%%%%%%%%%%%%%%% Figure 3 %%%%%%%%%%%%%%%%%%%%%%%%%%%%%%%%%%%%%%%%%%%%%%%%%%%%%%%%%%%%%%%%%%%%%%%%%%%
144 susceptFracVec = 0:0.02:1;
145 R0vec = 2;
146 colorVec = jet(length(R0vec));
147 transmissionReduction = 0:0.02:1;
148
149 % SIR model parameters
150 gamma = 1; % Recovery rate
151 lambda1 = 100; % Rate of susceptibles with lower tolerance to switch to
      masked class
152 delta1 = .1; % Rate of masked class with lower tolerance for adoption to
      remove intervention (mask) to return to susceptible class
153 lambda2 = 1; % Rate of susceptibles with higher tolerance to switch to
      masked class
154 delta2 = .1; % Rate of masked class with higher tolerance for adoption to
      remove intervention (mask) to return to susceptible class
155
156 recoveredFracVec = zeros(length(susceptFracVec), length(
      transmissionReduction), length(R0vec));
157 xVec = zeros(length(susceptFracVec), length(transmissionReduction), length(
      R0vec));
158 effectivenessVec = zeros(length(susceptFracVec), length(
      transmissionReduction), length(R0vec));
159
160 for z = 1:length(R0vec)
161     for y = 1:length(transmissionReduction)
162         for x = 1:length(susceptFracVec)

```

```

163         recoveredFracVec(x,y,z) = plotSIRDynamics(susceptFracVec(x),
            R0vec(z),transmissionReduction(y), 0, gamma, lambda1,
            delta1, lambda2, delta2, 1);
164     xVec(x,y,z) = susceptFracVec(x);
165     effectivenessVec(x,y,z) = transmissionReduction(y);
166     end
167     end
168 end
169
170 figure
171
172 subplot(1,2,1)
173 [x_new, e_new] = meshgrid(susceptFracVec, transmissionReduction);
174 contourf(x_new,e_new,recoveredFracVec(:,:,z)', 'LevelStep', 0.01)
175 xlabel('Fraction of Population with Low Risk Tolerance', 'FontSize', 14)
176 ylabel('Effectiveness of Intervention (\epsilon)', 'FontSize', 14)
177 h = colorbar;
178 title(h, 'Epidemic Size', 'FontSize', 14)
179 title(['R_0=', num2str(R0vec(z)), ', \lambda_1=', num2str(lambda1), ', \
            delta_1=', num2str(delta1), ', \lambda_2=', num2str(lambda2), ', \
            delta_2=', num2str(delta2)]);
180
181 hold on
182 points_x = [0.05, 0.2,.9, 0.5, .95, .75];
183 points_y = [0.8, 0.1, .2,0.9, .95, .5];
184
185 scatter(points_x, points_y, 'r', 'filled')
186
187 labels = {'A', 'B', 'C', 'D', 'E', 'F'};
188 text(points_x, points_y, labels, 'Color', 'red', 'VerticalAlignment', '
            bottom', 'HorizontalAlignment', 'right')
189
190 subplot(1,2,2)
191
192 hold on
193 for a = 1:length(points_x)
194     plotSIRDynamics(points_x(a), R0vec(z),points_y(a), 2, gamma, lambda1,
            delta1, lambda2, delta2, 1);
195 end
196
197 points_x = [0.45,0.4, .36, .85, .95, 0.72];
198 points_y = [0.025,0.13, 0.02,.01, .002, 0.02];
199
200 scatter(points_x, points_y, 'Marker', 'none')
201 labels = {'A', 'B', 'C', 'D', 'E', 'F'};
202 text(points_x, points_y, labels, 'Color', 'red', 'VerticalAlignment', '
            bottom', 'HorizontalAlignment', 'right')
203
204
205 %%%%%%%%%%%%%%%%%%%%%%%%%%%%%%%%%%%%%%%%%%%%%%%%%%%%%%%%%%%%%%%%%%%%%%%%%%% Figure 4 and S3 %%%%%%%%%%%%%%%%%%%%%%%%%%%%%%%%%%%%%%%%%%%%%%%%%%%%%%%%%%%%%%%%%%%%%%%%%%%
206 % Repeat for different parameter conditions to generate each panel
207
208 susceptFracVec = 0:0.01:1;
209 R0vec = 1:0.5:10;
210 colorVec = jet(length(R0vec));
211 transmissionReduction = 1;
212
213 % SIR model parameters
214 gamma = 1; % Recovery rate

```

```

215 lambda1 = 100; % Rate of susceptibles with lower tolerance to switch to
      masked class
216 delta1 = .1; % Rate of masked class with lower tolerance for adoption to
      remove intervention (mask) to return to susceptible class
217 lambda2 = 1; % Rate of susceptibles with higher tolerance to switch to
      masked class
218 delta2 = .1; % Rate of masked class with higher tolerance for adoption to
      remove intervention (mask) to return to susceptible class
219
220
221 recoveredFracVec = zeros(length(R0vec),length(susceptFracVec));
222 figure
223 hold on
224 for y = 1:length(R0vec)
225     for x = 1:length(susceptFracVec)
226         recoveredFracVec(y, x) = plotSIRDynamics(susceptFracVec(x), R0vec(
                y),transmissionReduction, 0, gamma, lambda1, delta1, lambda2,
                delta2, 1);
227     end
228     hold on
229     plot(susceptFracVec, recoveredFracVec(y,:), 'Color', colorVec(y,:), '
            LineWidth',2.5)
230 end
231
232 xlabel('Fraction of Population that are Risk Averse', 'FontSize', 14)
233 ylabel('Epidemic Size', 'FontSize', 14)
234 title(['\epsilon=',num2str(transmissionReduction), ', \lambda_1=',num2str(
            lambda1), ', \delta_1=',num2str(delta1), ', \lambda_2=',num2str(lambda2),
            ', \delta_2=',num2str(delta2)]);
235 hLegend = legend(string(R0vec), 'Location', 'eastoutside', 'FontSize', 12)
            ;
236 title(hLegend, 'R_0')
237
238 %%%%%%%%%%%%%%%%%%%%%%%%%%%%%%%%%%%%%%%%%%%%%%%%%%%%%%%%%%%%%%%%%%%%%%%%%%% Figure 5 %%%%%%%%%%%%%%%%%%%%%%%%%%%%%%%%%%%%%%%%%%%%%%%%%%%%%%%%%%%%%%%%%%%%%%%%%%%
239 % Repeat for different parameter conditions to generate each panel
240
241 figure
242 susceptFracVec = 0.2;
243 R0vec = 2;
244 colorVec = jet(length(R0vec));
245 transmissionReduction = .7;
246
247 % SIR model parameters
248 cVec = [0.01:0.01:1];
249 lambdaAvg = [0.5, 1:1:100];
250 gamma = 1; % Recovery rate
251 delta1 = .5; % Rate of masked class with lower tolerance for adoption to
      remove intervention (mask) to return to susceptible class
252 delta2 = .5; % Rate of masked class with higher tolerance for adoption to
      remove intervention (mask) to return to susceptible class
253
254 recoveredFracVec = zeros(length(cVec),length(lambdaAvg));
255
256 for x = 1:length(cVec)
257     for y = 1:length(lambdaAvg)
258         recoveredFracVec(x,y) = plotSIRDynamics(susceptFracVec, R0vec,
                transmissionReduction, 0, gamma, lambdaAvg(y)/(cVec(x)^(
                susceptFracVec/(1-susceptFracVec))), delta1, cVec(x)*lambdaAvg(
                y), delta2, 1);

```



```

259     end
260 end
261
262 [c_new, l_new] = meshgrid(cVec, lambdaAvg);
263 contourf(c_new, l_new, recoveredFracVec, 'LevelStep', 0.01)
264 xlabel('\lambda Homogeneity Index', 'FontSize', 14)
265 ylabel('\lambda_{Geometric Average}', 'FontSize', 14)
266 h = colorbar;
267 title(h, 'Epidemic Size', 'FontSize', 14)
268 title(['R_0=', num2str(R0vec), ', x_1=', num2str(susceptFracVec), ', \
epsilon=', num2str(transmissionReduction), ', \delta_1=', num2str(
delta1), ', \delta_2=', num2str(delta2)]);
269
270 %%%%%%%%%%%%%%%%%%%%%%%%%%%%%%%%%%%%%%%%%%%%%%%%%%%%%%%%%%%%%%%%%%%%%%%%% Figure 6 %%%%%%%%%%%%%%%%%%%%%%%%%%%%%%%%%%%%%%%%%%%%%%%%%%%%%%%%%%%%%%%%%%%%%%%%%
271
272 figure
273 subplot(1,2,1)
274
275 susceptFracVec = 0:0.01:1;
276 R0vec = 1:0.5:7;
277 colorVec = jet(length(R0vec));
278 transmissionReduction = 1;
279
280 % SIR model parameters
281 gamma = 1; % Recovery rate
282 lambda1 = 10; % Rate of susceptibles with lower tolerance to switch to
masked class
283 delta1 = .1; % Rate of masked class with lower tolerance for adoption to
remove intervention (mask) to return to susceptible class
284 lambda2 = .5; % Rate of susceptibles with higher tolerance to switch to
masked class
285 delta2 = .1; % Rate of masked class with higher tolerance for adoption to
remove intervention (mask) to return to susceptible class
286
287
288 recoveredFracVec = zeros(length(R0vec), length(susceptFracVec));
289 figure
290 hold on
291 for y = 1:length(R0vec)
292     for x = 1:length(susceptFracVec)
293         recoveredFracVec(y, x) = plotSIRDynamics(susceptFracVec(x), R0vec(
y), transmissionReduction, 0, gamma, lambda1, delta1, lambda2,
delta2, 1);
294     end
295     hold on
296     plot(susceptFracVec, recoveredFracVec(y,:), 'Color', colorVec(y,:), '
LineWidth', 2.5)
297 end
298
299 xlabel('Fraction of Population that are Risk Averse', 'FontSize', 14)
300 ylabel('Epidemic Size', 'FontSize', 14)
301 title(['\epsilon=', num2str(transmissionReduction), ', \lambda_1=', num2str(
lambda1), ', \delta_1=', num2str(delta1), ', \lambda_2=', num2str(lambda2),
', \delta_2=', num2str(delta2)]);
302 hLegend = legend(string(R0vec), 'Location', 'eastoutside', 'FontSize', 12)
;
303 title(hLegend, 'R_0')
304
305 susceptFracVec = 0:0.02:1;

```

```

306 R0vec = 2.5; % Only pick one R0 to show the surface plot for. Use other
      plot to pick the value of interest
307 colorVec = jet(length(R0vec));
308 transmissionReduction = 0:0.02:1;
309
310 recoveredFracVec = zeros(length(susceptFracVec),length(
      transmissionReduction),length(R0vec));
311 xVec = zeros(length(susceptFracVec),length(transmissionReduction),length(
      R0vec));
312 effectivenessVec = zeros(length(susceptFracVec),length(
      transmissionReduction),length(R0vec));
313
314 for z = 1:length(R0vec)
315     for y = 1:length(transmissionReduction)
316         for x = 1:length(susceptFracVec)
317             recoveredFracVec(x,y,z) = plotSIRDynamics(susceptFracVec(x),
                  R0vec(z),transmissionReduction(y), 0, gamma, lambda1,
                  delta1, lambda2, delta2, 1);
318             xVec(x,y,z) = susceptFracVec(x);
319             effectivenessVec(x,y,z) = transmissionReduction(y);
320         end
321     end
322 end
323
324 [X,Y,Z] = meshgrid(susceptFracVec,transmissionReduction,R0vec);
325
326 subplot(1,2,2)
327 for z = 1:length(R0vec)
328     surf(X(:,:,z), Y(:,:,z), recoveredFracVec(:,:,z), recoveredFracVec
          (:,:,z), 'FaceAlpha', 0.8, 'EdgeColor', 'interp');
329     hold on
330 end
331
332 xlabel('Fraction of Population that are Risk-Averse', 'FontSize', 14)
333 ylabel('Effectiveness of Intervention (\epsilon)', 'FontSize', 14)
334 zlabel('Epidemic Size', 'FontSize', 14)
335 title(['\lambda_1=', num2str(lambda1), ', \delta_1=', num2str(delta1), ',
          \lambda_2=', num2str(lambda2), ', \delta_2=', num2str(delta2)]);
336
337
338 %%%%%%%%%%%%%%%%%%%%%%%%%%%%%%%%%%%%%%%%%%%%%%%%%%%%%%%%%%%%%%%%%%%%%%%%%%% Figure 7 %%%%%%%%%%%%%%%%%%%%%%%%%%%%%%%%%%%%%%%%%%%%%%%%%%%%%%%%%%%%%%%%%%%%%%%%%%%
339
340 maskPolicyDataVsCases = readtable('maskPolicyDataVsCases.xlsx');
341
342 dates = datetime(maskPolicyDataVsCases.Date, 'InputFormat', '
      your_date_format'); % Replace 'your_date_format' with the actual format
343 policy = maskPolicyDataVsCases.MaskPolicyLevel;
344 cases = maskPolicyDataVsCases.ConfirmedNewCases;
345
346 figure;
347
348 % Plot the first variable on the left y-axis
349 yyaxis left;
350 plot(dates, policy);
351 ylabel('Mask Policy Level');
352 grid off;
353 ylim([0, 5]); % Uncomment and adjust if you need specific limits for the
      left y-axis
354

```

```

355 % Plot the second variable on the right y-axis
356 yyaxis right;
357 plot(dates, cases);
358 ylabel('Confirmed New Cases in USA');
359
360
361 datetick('x', 'yyyy-mm-dd');
362 xlabel('Date');
363 legend('Mask Policy Level', 'Confirmed New Cases');
364
365
366 %%%%%%%%%%%%%%%%%%%%%%%%%%%%%%%%%%%%%%%%%%% Figure S1 %%%%%%%%%%%%%%%%%%%%%%%%%%%%%%%%%%%%%%%%%%%
367
368 susceptFracVec = 0:0.02:1;
369 R0vec = 2;
370 colorVec = jet(length(R0vec));
371 transmissionReduction = 0:0.02:1;
372
373 % SIR model parameters
374 gamma = 1; % Recovery rate
375 lambda1 = 100; % Rate of susceptibles with lower tolerance to switch to
    masked class
376 delta1 = .1; % Rate of masked class with lower tolerance for adoption to
    remove intervention (mask) to return to susceptible class
377 lambda2 = 1; % Rate of susceptibles with higher tolerance to switch to
    masked class
378 delta2 = .1; % Rate of masked class with higher tolerance for adoption to
    remove intervention (mask) to return to susceptible class
379
380 recoveredFracVec = zeros(length(susceptFracVec),length(
    transmissionReduction),length(R0vec));
381 xVec = zeros(length(susceptFracVec),length(transmissionReduction),length(
    R0vec));
382 effectivenessVec = zeros(length(susceptFracVec),length(
    transmissionReduction),length(R0vec));
383
384 for z = 1:length(R0vec)
385     for y = 1:length(transmissionReduction)
386         for x = 1:length(susceptFracVec)
387             recoveredFracVec(x,y,z) = plotSIRDynamics(susceptFracVec(x),
                R0vec(z),transmissionReduction(y), 0, gamma, lambda1,
                delta1, lambda2, delta2, 0); % individuals adopt based on
                incidence
388             xVec(x,y,z) = susceptFracVec(x);
389             effectivenessVec(x,y,z) = transmissionReduction(y);
390         end
391     end
392 end
393
394
395 figure
396
397 subplot(1,2,1)
398 [x_new, e_new] = meshgrid(susceptFracVec, transmissionReduction);
399 contourf(x_new,e_new,recoveredFracVec(:,:,z)', 'LevelStep', 0.01)
400 xlabel('Fraction of Population with Low Risk Tolerance', 'FontSize', 14)
401 ylabel('Effectiveness of Intervention (\epsilon)', 'FontSize', 14)
402 h = colorbar;
403 title(h, 'Epidemic Size', 'FontSize', 14)

```

```

404 title(['R_0=', num2str(R0vec(z)), ', \lambda_1=', num2str(lambda1), ', \
      delta_1=', num2str(delta1), ', \lambda_2=', num2str(lambda2), ', \
      delta_2=', num2str(delta2)]);
405
406 hold on
407 points_x = 0.6*ones(100,1);
408 points_y = rand(100,1);
409
410 scatter(points_x, points_y, 'r', 'filled')
411
412 subplot(1,2,2)
413
414 for a = 1:length(points_x)
415     plotSIRDynamics(points_x(a), R0vec(z), points_y(a), 1, gamma, lambda1,
      delta1, lambda2, delta2, 0); % individuals adopt based on
      incidence
416 end
417
418
419 %%%%%%%%%%%%%%%%%%%%%%%%%%%%%%%%%%%%%%%%%%%%%%%%%%%%%%%%%%%%%%%%%%%%%%%%%%% Figure S2 %%%%%%%%%%%%%%%%%%%%%%%%%%%%%%%%%%%%%%%%%%%%%%%%%%%%%%%%%%%%%%%%%%%%%%%%%%%
420
421 susceptFracVec = 0:0.02:1;
422 R0vec = 2;
423 colorVec = jet(length(R0vec));
424 transmissionReduction = 0:0.02:1;
425
426 % SIR model parameters
427 gamma = 1; % Recovery rate
428 lambda1 = 100; % Rate of susceptibles with lower tolerance to switch to
      masked class
429 delta1 = .1; % Rate of masked class with lower tolerance for adoption to
      remove intervention (mask) to return to susceptible class
430 lambda2 = 1; % Rate of susceptibles with higher tolerance to switch to
      masked class
431 delta2 = .1; % Rate of masked class with higher tolerance for adoption to
      remove intervention (mask) to return to susceptible class
432
433 recoveredFracVec = zeros(length(susceptFracVec), length(
      transmissionReduction), length(R0vec));
434 xVec = zeros(length(susceptFracVec), length(transmissionReduction), length(
      R0vec));
435 effectivenessVec = zeros(length(susceptFracVec), length(
      transmissionReduction), length(R0vec));
436
437 for z = 1:length(R0vec)
438     for y = 1:length(transmissionReduction)
439         for x = 1:length(susceptFracVec)
440             recoveredFracVec(x,y,z) = plotSIRDynamics(susceptFracVec(x),
      R0vec(z), transmissionReduction(y), 0, gamma, lambda1,
      delta1, lambda2, delta2, 0); % individuals adopt based on
      incidence
441             xVec(x,y,z) = susceptFracVec(x);
442             effectivenessVec(x,y,z) = transmissionReduction(y);
443         end
444     end
445 end
446
447
448 figure

```

```

449
450 subplot(1,2,1)
451 [x_new, e_new] = meshgrid(susceptFracVec, transmissionReduction);
452 contourf(x_new,e_new,recoveredFracVec(:,:,z)', 'LevelStep', 0.01)
453 xlabel('Fraction of Population with Low Risk Tolerance', 'FontSize', 14)
454 ylabel('Effectiveness of Intervention (\epsilon)', 'FontSize', 14)
455 h = colorbar;
456 title(h, 'Epidemic Size', 'FontSize', 14)
457 title(['R_0=', num2str(R0vec(z)), ', \lambda_1=', num2str(lambda1), ', \
      delta_1=', num2str(delta1), ', \lambda_2=', num2str(lambda2), ', \
      delta_2=', num2str(delta2)]);
458
459 hold on
460 points_x = rand(100,1);
461 points_y = 0.3*ones(100,1);
462
463 scatter(points_x, points_y, 'r', 'filled')
464
465 subplot(1,2,2)
466
467 for a = 1:length(points_x)
468     plotSIRDynamics(points_x(a), R0vec(z),points_y(a), 1, gamma, lambda1,
469         delta1, lambda2, delta2, 0); % individuals adopt based on incidence
470 end
471 %%%%%%%%%%%%%%%%%%%%%%%%%%%%%%%%%%%%%%%%%%%%%%%%%%%%%%%%%%%%%%%%%%%%%%%%%%% Figure S4 %%%%%%%%%%%%%%%%%%%%%%%%%%%%%%%%%%%%%%%%%%%%%%%%%%%%%%%%%%%%%%%%%%%%%%%%%%%
472
473 susceptFracVec = 0:0.02:1;
474 R0vec = 2;
475 colorVec = jet(length(R0vec));
476 transmissionReduction = 0:0.02:1;
477
478 % SIR model parameters
479 gamma = 1; % Recovery rate
480 lambda1 = 100; % Rate of susceptibles with lower tolerance to switch to
      masked class
481 delta1 = .1; % Rate of masked class with lower tolerance for adoption to
      remove intervention (mask) to return to susceptible class
482 lambda2 = 1; % Rate of susceptibles with higher tolerance to switch to
      masked class
483 delta2 = .1; % Rate of masked class with higher tolerance for adoption to
      remove intervention (mask) to return to susceptible class
484
485 recoveredFracVec = zeros(length(susceptFracVec),length(
      transmissionReduction),length(R0vec));
486 xVec = zeros(length(susceptFracVec),length(transmissionReduction),length(
      R0vec));
487 effectivenessVec = zeros(length(susceptFracVec),length(
      transmissionReduction),length(R0vec));
488
489 for z = 1:length(R0vec)
490     for y = 1:length(transmissionReduction)
491         for x = 1:length(susceptFracVec)
492             recoveredFracVec(x,y,z) = plotSIRDynamics(susceptFracVec(x),
493                 R0vec(z),transmissionReduction(y), 0, gamma, lambda1,
494                 delta1, lambda2, delta2, 1); % individuals adopt based on
495                 infection level
496             xVec(x,y,z) = susceptFracVec(x);
497             effectivenessVec(x,y,z) = transmissionReduction(y);

```

```

495         end
496     end
497 end
498
499
500 figure
501
502 subplot(1,2,1)
503 [x_new, e_new] = meshgrid(susceptFracVec, transmissionReduction);
504 contourf(x_new,e_new,recoveredFracVec(:,:,z)', 'LevelStep', 0.01)
505 xlabel('Fraction of Population with Low Risk Tolerance', 'FontSize', 14)
506 ylabel('Effectiveness of Intervention (\epsilon)', 'FontSize', 14)
507 h = colorbar;
508 title(h, 'Epidemic Size', 'FontSize', 14)
509 title(['R_0=', num2str(R0vec(z)), ', \lambda_1=', num2str(lambda1), ', \
        delta_1=', num2str(delta1), ', \lambda_2=', num2str(lambda2), ', \
        delta_2=', num2str(delta2)]);
510
511 hold on
512 points_x = 0.6*ones(100,1);
513 points_y = rand(100,1);
514
515 scatter(points_x, points_y, 'r', 'filled')
516
517 subplot(1,2,2)
518
519 for a = 1:length(points_x)
520     plotSIRDynamics(points_x(a), R0vec(z),points_y(a), 1, gamma, lambda1,
521         delta1, lambda2, delta2, 1); % individuals adopt based on infection
522         level
521 end
522
523
524 %%%%%%%%%%%%%%%%%%%%%%%%%%%%%%%%%%%%%%%%%%%%%%%%%%%%%%%%%%%%%%%%%%%%%%%%%%% Figure S5 %%%%%%%%%%%%%%%%%%%%%%%%%%%%%%%%%%%%%%%%%%%%%%%%%%%%%%%%%%%%%%%%%%%%%%%%%%%
525
526 susceptFracVec = 0:0.02:1;
527 R0vec = 2;
528 colorVec = jet(length(R0vec));
529 transmissionReduction = 0:0.02:1;
530
531 % SIR model parameters
532 gamma = 1; % Recovery rate
533 lambda1 = 100; % Rate of susceptibles with lower tolerance to switch to
534     masked class
535 delta1 = .1; % Rate of masked class with lower tolerance for adoption to
536     remove intervention (mask) to return to susceptible class
537 lambda2 = 1; % Rate of susceptibles with higher tolerance to switch to
538     masked class
539 delta2 = .1; % Rate of masked class with higher tolerance for adoption to
540     remove intervention (mask) to return to susceptible class
541
542 recoveredFracVec = zeros(length(susceptFracVec),length(
543     transmissionReduction),length(R0vec));
544 xVec = zeros(length(susceptFracVec),length(transmissionReduction),length(
545     R0vec));
546 effectivenessVec = zeros(length(susceptFracVec),length(
547     transmissionReduction),length(R0vec));
548
549 for z = 1:length(R0vec)

```

```

543     for y = 1:length(transmissionReduction)
544         for x = 1:length(susceptFracVec)
545             recoveredFracVec(x,y,z) = plotSIRDynamics(susceptFracVec(x),
                    R0vec(z),transmissionReduction(y), 0, gamma, lambda1,
                    delta1, lambda2, delta2, 1); % individuals adopt based on
                    infection level
546             xVec(x,y,z) = susceptFracVec(x);
547             effectivenessVec(x,y,z) = transmissionReduction(y);
548         end
549     end
550 end
551
552
553 figure
554
555 subplot(1,2,1)
556 [x_new, e_new] = meshgrid(susceptFracVec, transmissionReduction);
557 contourf(x_new,e_new,recoveredFracVec(:,:,z)', 'LevelStep', 0.01)
558 xlabel('Fraction of Population with Low Risk Tolerance', 'FontSize', 14)
559 ylabel('Effectiveness of Intervention (\epsilon)', 'FontSize', 14)
560 h = colorbar;
561 title(h, 'Epidemic Size', 'FontSize', 14)
562 title(['R_0=', num2str(R0vec(z)), ', \lambda_1=', num2str(lambda1), ', \
        delta_1=', num2str(delta1), ', \lambda_2=', num2str(lambda2), ', \
        delta_2=', num2str(delta2)]);
563
564 hold on
565 points_x = rand(100,1);
566 points_y = 0.3*ones(100,1);
567
568 scatter(points_x, points_y, 'r', 'filled')
569
570 subplot(1,2,2)
571
572 for a = 1:length(points_x)
573     plotSIRDynamics(points_x(a), R0vec(z),points_y(a), 1, gamma, lambda1,
                    delta1, lambda2, delta2, 1); % individuals adopt based on infection
                    level
574 end
575
576
577
578 %%%%%%%%%%%%%%%%%%%%%%%%%%%%%%%%%%%%%%%%%%%%%%%%%%%%%%%%%%%%%%%%%%%%%%%%%%% Figure S6 %%%%%%%%%%%%%%%%%%%%%%%%%%%%%%%%%%%%%%%%%%%%%%%%%%%%%%%%%%%%%%%%%%%%%%%%%%%
579 % Repeat this script with corresponding parameters to generate each panel
580
581 figure
582 susceptFracVec = 0.2;
583 R0vec = 2;
584 colorVec = jet(length(R0vec));
585 transmissionReduction = .7;
586
587 % SIR model parameters
588 cVec = [0.01:0.05:1];
589 lambdaAvg = [0.5, 1:5:100];
590 gamma = 1; % Recovery rate
591 delta1 = .5; % Rate of masked class with lower tolerance for adoption to
        remove intervention (mask) to return to susceptible class
592 delta2 = .5; % Rate of masked class with higher tolerance for adoption to
        remove intervention (mask) to return to susceptible class

```

```

593
594 recoveredFracVec = zeros(length(cVec),length(lambdaAvg));
595
596 for x = 1:length(cVec)
597     for y = 1:length(lambdaAvg)
598         recoveredFracVec(x,y) = plotSIRDynamics(susceptFracVec, R0vec,
            transmissionReduction, 0, gamma, lambdaAvg(y)*(1-susceptFracVec
            *cVec(x))/(1-susceptFracVec), delta1, cVec(x)*lambdaAvg(y),
            delta2, 1); %Arithmetic parameterization
599     end
600 end
601
602 [c_new, l_new] = meshgrid(cVec, lambdaAvg);
603 contourf(c_new,l_new,recoveredFracVec', 'LevelStep', 0.01)
604 xlabel('\lambda Homogeneity Index', 'FontSize', 14)
605 ylabel('\lambda_{Arithmetic Average}', 'FontSize', 14)
606 h = colorbar;
607 title(h, 'Epidemic Size', 'FontSize', 14)
608 title(['R_0=', num2str(R0vec), ', x_1=', num2str(susceptFracVec), ', \
        epsilon=', num2str(transmissionReduction), ', \delta_1=', num2str(
        delta1), ', \delta_2=', num2str(delta2)]);

```